Journal of
Nuclear Engineering

MDPI

Article

Spent Nuclear Fuel—Waste to Resource, Part 1: Effects of Post-Reactor Cooling Time and Novel Partitioning Strategies in Advanced Reprocessing on Highly Active Waste Volumes in Gen III(+) UOx Fuel Systems

Alistair F. Holdsworth [1,*], Edmund Ireland [1] and Harry Eccles [2]

[1] Department of Chemical Engineering, University of Manchester, Oxford Road, Manchester M13 9PL, UK; edmund.ireland@manchester.ac.uk
[2] School of Pharmacy and Biomedical Sciences, University of Lancashire, Fylde Road, Preston PR1 2HE, UK; heccles2@uclan.ac.uk
* Correspondence: alistair.holdsworth@manchester.ac.uk

Abstract

Some of nuclear power's primary detractors are the unique environmental challenges and impacts of radioactive wastes generated during fuel cycle operations. Key benefits of spent fuel reprocessing (SFR) are reductions in primary high active waste (HAW) masses, volumes, and lengths of radiotoxicity at the expense of secondary waste generation and high capital and operational costs. By employing advanced waste management and resource recovery concepts in SFR beyond the existing standard PUREX process, such as minor actinide and fission product partitioning, these challenges could be mitigated, alongside further reductions in HAW volumes, masses, and duration of radiotoxicity. This work assesses various current and proposed SFR and fuel cycle options as base cases, with further options for fission product partitioning of the high heat radionuclides (HHRs), rare earths, and platinum group metals investigated. A focus on primary waste outputs and the additional energy that could be generated by the reprocessing of high-burnup PWR fuel from Gen III(+) reactors using a simple fuel cycle model is used; the effects of 5- and 10-year spent fuel cooling times before reprocessing are explored. We demonstrate that longer cooling times are preferable in all cases except where short-lived isotope recovery may be desired, and that the partitioning of high-heat fission products (Cs and Sr) could allow for the reclassification of traditional raffinates to intermediate level waste. Highly active waste volume reductions approaching 50% vs. PUREX raffinate could be achieved in single-target partitioning of the inactive and low-activity rare earth elements, and the need for geological disposal could potentially be mitigated completely if HHRs are separated and utilised.

Keywords: spent nuclear fuel; waste to resource; waste management; resource recovery; nuclear fuel cycle; spent fuel reprocessing; partitioning and transmutation; circular economy; sustainability

Academic Editor: Dan Gabriel Cacuci

Received: 21 April 2025
Revised: 17 July 2025
Accepted: 25 July 2025
Published: 5 August 2025

Citation: Holdsworth, A.F.; Ireland, E.; Eccles, H. Spent Nuclear Fuel—Waste to Resource, Part 1: Effects of Post-Reactor Cooling Time and Novel Partitioning Strategies in Advanced Reprocessing on Highly Active Waste Volumes in Gen III(+) UOx Fuel Systems. *J. Nucl. Eng.* **2025**, *6*, 29. https://doi.org/10.3390/jne6030029

1. Introduction

Despite the potential to generate vast quantities of low-carbon energy, widespread adoption of nuclear power is hampered by high costs and concerns over the generation, processing, and disposal of vast quantities of many and varied past, present, and future

radioactive wastes generated in fuel cycle operations [1], alongside overall negative public perception arising from these and other factors, such as accidents [2,3]. Technologies such as spent nuclear fuel reprocessing (SFR) reduce the radiotoxicity and volume of hazardous material for disposal in addition to other nuclear fuel cycle (NFC) efficiency benefits [4], but high costs and proliferation concerns limit wider uptake of these operations. Reducing the costs of SFR and decreasing the waste volumes that arise from the NFC are two of the primary drivers in current fuel cycle research as interest in nuclear power increases in the face of increasing climate change and other global challenges, such as materials shortages [2].

Nuclear wastes arising from NFC operations occur in a wide range of forms and hazard classifications, the definitions of which vary appreciably from country to country [5]. For the purposes of this work, we shall consider the following:

- High-level waste (HLW) are typically defined as "appreciably heat generating", meaning that active cooling is often required. In Germany, this means a heat output of > 200 W/m^3 [5], which serves as a useful definition for this work. HLW includes materials such as spent nuclear fuel (SNF), reprocessing raffinates, some activated structural materials, etc., which must always be handled remotely due to their intense radiation fields, which are extremely hazardous if not lethal to unprotected humans, even after short exposure [5]. These wastes are often vitrified for long-term storage or disposal in a geological disposal facility (GDF), the latter of which has yet to be commercially realised anywhere at the time of writing [6].
- Intermediate-level waste (ILW) include materials such as the irradiated (zircalloy) cladding and structural elements from SNF assemblies, which are not appreciably heat-generating but nonetheless still highly radioactive. These require remote handling in shielded hot cells, but in contrast to HLW are typically prepared and stored for disposal in a cemented form without the necessity for continuous active cooling. Under UK legislation, ILW is defined as "neither HLW nor (very) low level waste".
- Low-level waste (LLW) and very low-level waste (VLLW) are of sufficiently low activity that they can be handled outside hot cells, and include materials such as contaminated PPE, demolition rubble from nuclear facilities, and some peripheral nuclear plant hardware.

Short of the questionably efficient transmutation to lower-level wastes in a reactor [7], nuclear wastes cannot be removed from existence, merely separated and/or partitioned from one place to another with varying degrees of difficulty. One detractor that could be levelled against the nuclear industry is that any material originating from fission is deemed to be harmful, regardless of the level of activity present, if any, to the detriment of recovering potential resources present therein [8,9]. Partitioning and/or recovery of certain wastes for use could, however, lead to numerous and significant benefits to the NFC, as will be discussed later [10,11].

This is evidenced by SNF containing a large number of inactive, naturally occurring isotopes produced inherently during fission that otherwise represent scarce and highly useful materials, such as the platinum group metals (PGMs), rare earth elements (REEs), and noble gases (NGs), alongside a significant number of harmful but also potentially useful isotopes [8]. The recovery of these materials from SNF as a value stream was proposed as far back as the 1960s [12] but is only now receiving significant attention in light of increased interest in nuclear power [13–16], though attitudes to the use of materials sourced from nuclear origins must change for greater acceptance [9].

The current PUREX (plutonium uranium reduction extraction) process, the gold standard in SFR employed around the world, only extracts U and Pu from SNF, leaving the fission products (FPs) and minor actinides (MAs) as wastes for disposal [4,17]. This results

in a marked reduction in waste volume, a significant reduction in mass relative to the disposal or storage of whole SNF assemblies, and a decrease in the length of radiotoxicity from Pu by several orders of magnitude (see Figure 1) [4]. Ideally, the Pu and U recovered are recycled for further energy generation as MOX (mixed oxide) fuel, rather than being stored. Developments of this, including the SANEX (selective actinide extraction) and GANEX (grouped actinide extraction), further partition the MAs (Np, Am, Cm, Bk, Cm) from SNF raffinate post-U and -Pu extraction to further reduce the length of radiotoxicity (see Figure 1) by fissioning these species in fast-spectrum reactors [4,17,18].

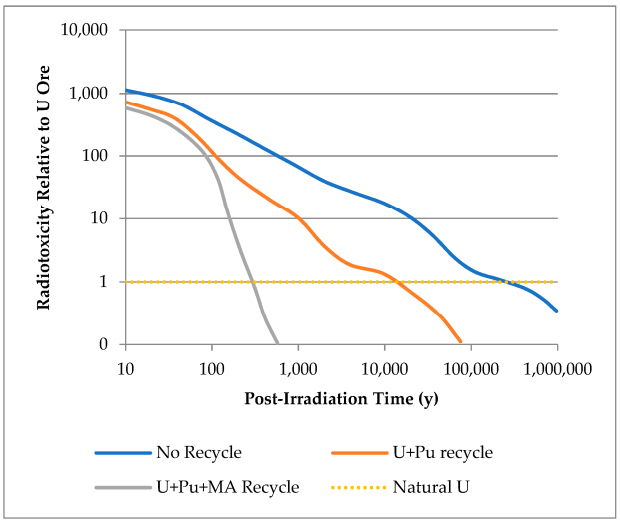

Figure 1. Reduction in length and intensity of radiotoxicity with Pu and U recycle, and additional MA partitioning and transmutation, relative to an open fuel cycle (no recycle) and natural uranium [18]. NB: axis scales are logarithmic.

Further to this, an advanced concept whereby the high-heat radionuclides (HHRs, the FPs ^{134}Cs, ^{137}Cs, and ^{90}Sr), the primary sources of radioactivity in SNF HLW, are selectively partitioned during reprocessing for separate storage and/or disposal [11]. This could potentially allow for reclassification of the remaining waste from HLW to ILW [13], and some recent efforts towards achieving this goal, with potential further benefits for SFR operations by addressing current operational challenges and high costs, have been undertaken by the authors [13–16]. More recently, it has been proposed to utilise SNF for the production of H_2 via radiolysis of water with a TiO_2 catalyst; separation and concentration of HHRs to facilitate this would likely increase the effectiveness of the process, which is potentially capable of generating the world's entire demand for hydrogen from current SNF stockpiles [10]. Although a radiolysis-based H_2 production process was proposed as far back as 1976 (based on HHRs in solution), this was concluded to be unviable at the time of publication [19], unlike the more recent proposal by Vandenborre and co-workers. This would effectively turn materials considered hazardous and inconvenient waste into a true resource and offset the high costs of the NFC, with great potential for the generation of economic return and environmental benefits.

In a similar vein, some recent research has been directed at the recovery of valuable and naturally scarce FPs from SNF during SFR to offset the high costs of these operations, providing sovereign sources of finite materials that are in high industrial demand [8,20,21]. This would, potentially, allow the NFC to become part of a greater material circular economy and significantly more sustainable in its operation [2,8,21]. Categories of material proposed for extraction include the platinum group metals (PGMs—Ru, Rh, Pd, Ag) and rare earth elements (REEs—Y, La-Tb); additionally, several useful radioisotopes are present in SNF and can potentially be extracted (e.g., ^{90}Sr/^{90}Y, ^{137}Cs, ^{85}Kr, etc.) [8,20–22].

The available literature contains comparatively little discussion on the impact of these processes (and combinations thereof) on reprocessing waste volumes and the NFC in general. Consequently, we present an assessment of these process impacts in the context of modern NFCs. This uses a simulated composition for high-burnup (HBU, 60 GWd/tHM) Gen III(+) pressurised water reactor (PWR) SNF (UO_2, 5% initial ^{235}U) from a reactor such as the EPR (European Pressurised water Reactor) [23]. This fuel will be assumed to have been cooled for periods of either 5 or 10 years post-irradiation before reprocessing. Several options, including the open fuel cycle (Scenario 1), the UREX cycle (Scenario 2), the current PUREX cycle (Scenario 3), and the latter of these combined with minor actinide separations (Scenario 4), are explored for comparative purposes as base cases, with a primary focus on fission production separations recovering the HHRs (Scenario 5a), PGMs (Scenario 5b), and low-activity REEs (Scenario 5c) in separate scenarios. The base cases correspond to several explored options in studies conducted previously, which we shall refer readers to for comparison [24]. Using these values, we explore the effects of different reprocessing separation options on primary HLW volumes, masses, and activities from these operations. Although our source data [23] include information for comparative MOX SNF, we do not consider the use of Pu multi-recycle in this work [25–27], although this may be investigated in future publications.

2. Methodology

2.1. Data Sources and Calculations

The isotopic composition of the virtual SNF system was acquired from the work of Ando and Takano, pp. 121–135, using the 5- and 10-year post-reactor values provided [23]. These values were originally generated by the ORIGEN fuel performance code, amongst others, and represent one of the most comprehensive available sources of SNF compositions. These values were used to develop a statistical calculator in a previous work [28]. While we acknowledge there are more recent data sources available covering newer fuels and different reactor systems (including high-temperature gas-cooled reactors) [29,30], these often lack the detail, comprehensiveness, and consistency of the source data used for this work across such a wide range of reactors, fuel types, and irradiation histories, as previously discussed [28]. The full list of isotopes modelled for this work is presented in the Appendix A, see Tables A1 and A2.

Additional isotopic data (half-lives, specific activities, decay energies) were acquired from the IAEA isotope browser [31], NRC [32], and WISE Uranium project [33] databases. The complete list of isotopes included in the model for this work are presented in Table A1 (actinides and daughters) and Table A2 (fission products); the full dataset is available in the electronic lementary Materials (ESI) file. Some values were approximated for long-lived species where specific data were not available, and data for some isotopes are not included in the original source; some best-guess assumptions were made regarding the identities of undefined isotopes from the primary dataset, as outlined in the ESI.

Please note that the dataset used for this work does model a simplified representation of counterion (i.e., oxide, O^{2-}) activation (which starts from 100% ^{16}O, rather than natural composition) [23]. Furthermore, it does not provide information regarding ternary fission products, nor is alpha decay or neutron emission and capture beyond the reactor operation modelled [23]. These isotopes, being predominantly volatile (isotopes of H, He, Li, Be, B, C, N, O, F, and Ne), are not discussed further.

The specific decay heats for each isotope were calculated as a product of specific activity (Bq/g), concentration (g/tHM), and decay energy (keV). These isotope-specific heating powers were then summed to express a value per (metric) tonne of spent fuel. Please note than unlike our previous work [28], where the decays of short-lived daughters

(e.g., ^{90}Y and ^{106}Rh) were treated as being part of their parent for calculation purposes, here they are measured under the element of the intermediate, with the exception of ^{137m}Ba and the daughter products of nuclides undergoing double β^- decay.

The decay energies used for these calculations ($Q_\alpha/Q_\beta/Q_{EC}$, etc.) represent the total potential decay energy for each isotope [28]. While this is relatively accurate for nuclides that decay via alpha decay, this tends to somewhat overestimate decay heats for those that decay via beta–gamma emission and/or electron capture, as in these processes, a portion of the energy is lost to non-interacting antineutrino emission [28]. For the purposes of this work, however, we consider these values to be acceptable conservative estimates of true decay heat and radioactivity values. These estimates could be improved by accounting for minor decay branches, but these would render the calculations far more complex for limited benefit, and as such are omitted from this work.

2.2. Consideration of Separation Operations and Processes

For simplicity, we consider all physical and chemical separations that occur in a reprocessing facility to be simplified and idealised "black box" operations that function with 100% efficiency. While this is not wholly representative of real-world processes, most operators would aim to achieve near-quantitative recovery of target elements to justify the costs and environmental impacts of such operations. All operations are treated in this manner, including the head-end operations of reprocessing. This includes head-end processes that produce two primary waste streams, volatile fission products (Br, Kr, I, Xe) [34,35] and generic ILW composed of fuel cladding and fuel assembly hardware. The former of these is counted as a dedicated waste stream in each scenario, while the ILW stream must be discounted, as it is dominated by activation products that are out of the scope of our source dataset. Furthermore, the concentration, activity, and decay heat of U daughters (Pa, Th, Ac, Ra, Fr, Rn, At, Po, Bi, and Pb) are counted with U itself as, while these would be separated from the U during chemical reprocessing operations, these species reform a secular equilibrium over time during storage through natural decay of U. Conceptual head-end technologies for reprocessing, such as voloxidation, which have a significant impact on the routing of many FPs are not discussed, as these add further complication beyond the scope of this work. The simulated vitrified waste outputs from this work assume a glass density of 3.33 g/cm^3 and a waste loading of 20 wt% (accounting for oxides as the chemical form of waste elements, etc.) [36,37].

While we acknowledge that these are not necessarily the most dense wasteforms possible based upon more recent developments in this field [38–40], these values draw upon UK experience in HLW management with respect to loading, density, and so on. We feel that this would provide an adequate blend between wasteform density and heat loading in a potential GDF environment. We would refer readers to the cited references for a more thorough understanding of these; regardless of the waste management approach taken with respect to wasteform density and chemistry, we can assume that at a constant loading, the variations in activity between our different scenarios would remain constant and are thus comparable across a range of wasteforms.

The SNF + HLW masses from Wigeland et al. are included for comparison, with normalised values presented (relative to Scenario 1/EG01—open fuel cycle) [24]. These are not directly translated into HLW volumes, as we have done here, but nonetheless serve as a useful comparison; this was stated to omit the choice of waste from the discussion presented. Volumes of LLW are provided in this work, but these are not pertinent to the discussion here. No data are presented pertaining to fission product partitioning.

2.3. Spent Fuel Reprocessing Scenarios

We consider several NFC base cases and more conceptual scenarios incorporating a mixture of proposed and extant flowsheets for the reprocessing of SNF. A comprehensive review of the maturity of most of these technologies can be found in a recent review [17]. These scenarios are discussed below.

2.3.1. Scenario 1: The Open Fuel Cycle

The least-preferable approach to handling spent fuel is direct disposal following several decades of first wet storage and then dry-cask storage. This essentially removes valuable fissile and fertile materials from availability, alongside many other naturally scarce resources that have been identified [8,20]. In this case, the mass and volume of material for disposal are at least one order of magnitude higher than if any separative operations (outlined below) are performed on SNF. For our purposes, we shall assume the disposal of entire PWR SNF bundles in a hypothetical GDF.

2.3.2. Scenario 2: UREX for Waste Volume Reduction and/or U Re-Enrichment

One proposed approach to handling the volume of SNF currently in wet and dry storage around the world is to chemically separate and perhaps reuse U, the main component of SNF, from the remaining constituents, which are then disposed of as vitrified waste [41]. This would use an adaptation of the established solvent-extraction-based PUREX process commonly dubbed UREX (uranium extraction), with disposal of the remaining components, including Pu. A great many variations on the UREX process could further treat the waste raffinates to recover desirable materials through operations such as TALSPEAK and derivatives, none of which have yet made it to commercial operation [17], and the discussion of which is largely beyond the scope of this work. The materials for disposal in this scenario will be considered as 20 wt% vitrified composites in glass [37].

2.3.3. Scenario 3: The Traditional PUREX Process

Representing the current standard SNF reprocessing flowsheet around the world, the PUREX process was initially developed to recover Pu for nuclear weapon purposes. In modern times, however, this highly effective flowsheet is used to reprocess SNF by selectively separating the U and Pu present for use as MOX for further energy generation in modern reactors [17]. The HLW raffinate materials for disposal in this scenario will be considered as 20 wt% vitrified composites in glass [37].

2.3.4. Scenario 4: PUREX with Minor Actinide Separations, GANEX, or UREX Versions

The next evolution of the PUREX process proposed for several decades involves the use of additional separation processes or alternative flowsheets to partition the MAs (Np, Am, Cm) during operations, providing a dedicated feed of these materials for storage and later transmutation in a (fast-spectrum) reactor. This would serve to reduce the length and severity of radiotoxicity of reprocessing raffinates relative to PUREX. While there are several methods by which this could be achieved, such as the addition of the SANEX process to PUREX, the use of the dual-stage GANEX flowsheet, or UREX plus the various proposed TALSPEAK and similar operations [17], these are all functionally similar and, as such, will be treated as achieving the same end result for our purposes. The materials for disposal in this scenario will be considered as 20 wt% vitrified composites in glass [37].

2.3.5. Scenario 5a: U, Pu, and Minor Actinide Separations with HHR Removal

If the MAs are removed from SNF during reprocessing, the remaining highly active raffinate contains only FPs, of which the primary sources of radioactivity are, depending on post-reactor cooling time, ^{134}Cs, ^{137}Cs, ^{90}Sr (and ^{90}Y), ^{106}Ru (and ^{106}Rh), ^{144}Ce (and

^{144}Pr), ^{147}Pm, $^{154/155}$Eu, and ^{85}Kr. Forsberg proposed the removal of the first three of these using selective separations as a means to reduce decay heat loads on repositories by using separate decay storage of these nuclides [11], though they could be utilised for a number of potential applications instead. The existing proposals to achieve this would extract Cs and Sr selectively from reprocessing highly active raffinates, following the extraction of U, Pu, and the MAs. Our own research has demonstrated that this could, in theory, be achieved prior to these operations, to the benefit of all downstream processes [13–16]. The non-HHR materials for disposal in this scenario will be considered as 20 wt% vitrified composites in glass [37], while the forms for the HHRs themselves require special consideration, given the levels of decay heat produced when in a concentrated state [11].

2.3.6. Scenario 5b: U, Pu, and Minor Actinide Separations with PGM Recovery

As the PGMs are the most valuable elemental components of SNF after the actinides [8], recovering these during reprocessing could serve to offset a significant proportion of the high costs of these operations, as the concentrations of these elements in SNF are far higher than in any natural ore [12]. Proposals to achieve this have been proposed since the 1960s but have seen more recent attention, given geopolitical shifts, increasing demands for naturally scarce materials, and a range of other factors. We shall consider the separation and recovery of Ru, Rh, Pd, and Ag from the highly active raffinate outputs of reprocessing, with disposal of the remaining FPs. The materials for disposal in this scenario will be considered as 20 wt% vitrified composites in glass [37]. The potential necessity for the decay storage or separated PGMs is also discussed.

2.3.7. Scenario 5c: U, Pu, and Minor Actinide Separations with REE Recovery

Similar to the PGMs, the REEs are naturally scarce, experiencing exponentially increasing demands from modern high technologies, and occur at high concentrations in SNF [8,20,23]. Most MA separation technologies also co-separate the chemically similar REEs before selectively stripping the lanthanides and actinides [17]. As the REEs occur together naturally and are mined at scale around the world, technologies to separate these chemically similar elements using chromatographic approaches are robust and could be applied to REE streams from SNF reprocessing. Several of the REEs found in SNF possess no radioactive isotopes (when certain short-lived daughter nuclides are discounted) or are essentially non-radioactive, and as such, these could be used directly without the need for decay storage. The various options for the REE stream will be analysed. The materials for disposal in this scenario will be considered as 20 wt% vitrified composites in glass [37].

3. Results and Discussion

Scenarios 1 to 4 represent the current implementations and state-of-the-art proposals for handling SNF in the NFC. These, Scenario 4 in particular, provide the basis for the more advanced concepts discussed in Scenarios 5a to 5c, as we assume any new-build SFR plant will include, at a minimum, primary U and Pu and secondary MA separations. These scenarios are discussed in detail with comparisons following this.

3.1. Scenario 1: The Open Fuel Cycle

The least favourable approach to the NFC is the open fuel cycle (Figure 2), followed by the "wait and see" method used by many nuclear-generating countries. Disposing of SNF directly after use, following a period of post-reactor cooling, is wasteful, inefficient, and, in the long term, unsustainable [2]. This also represents the least-efficient disposal option in terms of waste mass and volume, as, in addition to the bulk U component of SNF, all of the metallic components of the cladding and fuel assemblies are retained for disposal, in addition to the air gaps between fuel pins and necessary separation between

bundles for appropriate cooling and for criticality safety. The proposed direct SNF bundle disposal approach proposed by several nations (Sweden, Finland) further uses alarming volumes of strategic materials such as copper, and as such is highly unfavourable, in addition to potentially requiring longer cooling times before final disposal (25–30 years) than reprocessed SNF wastes (5–10 years). For comparison with prior works, please see the data published in the extensive report by Wigeland et al. [24], where this scenario corresponds to EG01 (once through using enriched-U fuel in thermal critical reactors) outlined therein. We would also refer readers to the work of Acar and Zaonuglu for a more detailed modelling of this proposed SNF disposal route [42].

Figure 2. Simplified schematic summary of the open fuel cycle and the "wait and see" approach.

Using the values from Roddy et al. [43], a standard 17 × 17 PWR fuel assembly contains 461.4 kg of U as the initial heavy metal mass (as 523.4 kg of UO_2), alongside 134.5 kg of zircalloy and other metals, occupying a nominal volume of 0.186 m^3 externally. This means that per ton of initial heavy metal, a total of 1446 kg of mass must be disposed of, occupying a volume of at least 0.403 m^3, and likely much more than this given the necessity to space fuel bundles for criticality and decay heat safety and the additional volume occupied by the waste disposal canisters: we can assume a value of at least double or triple this (based on the image from [44]). The high density of U (present as UO_2) is a major contributor to the wasteform's physical properties in this scenario. The mass of the wasteform would also be significantly greater due to the volume of copper, steel, and/or concrete used to contain the fuel bundles.

Where disposal in a GDF is not implemented, but instead the SNF is contained in dry casks for an extended period in the "wait and see" approach is more preferable but still less than ideal, as useful fissile and fertile nuclides are essentially removed from available supplies for the interim but could, at some cost, be recovered for later reprocessing or recycle.

3.2. Scenario 2: The UREX Process

The base UREX process (Figure 3) is an adaptation of the PUREX process, whereby Pu is not co-extracted alongside U in the primary solvent extraction operation, leaving a raffinate containing all the remaining components of SNF, including all transuranics and FPs. This raffinate is then vitrified and containerised for storage until deep geological disposal in a GDF can be undertaken, while the U is either stored for disposal at a lower-level classification or could be re-enriched for further energy generation. The respective masses, activities, and decay heats of these two streams from our simulated HBU PWR SNF are presented in Table 1.

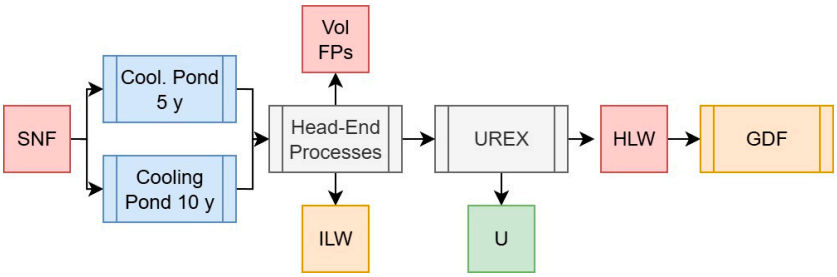

Figure 3. Simplified schematic summary of the UREX process, with SNF input and the primary outputs of this operation.

Table 1. Scenario 2 data, including feed masses, activities, decay heats, and specific decay heats. The values for the daughters of U are included with it.

	Masses (g/tiHM)		**Activity (Bq/tiHM)**		**Decay Heat (W/tiHM)**		**Specific DH (W/gHM)**	
Feed	5 y	10 y	5 y	10 y	5 y	10 y	5 y	10 y
U	9.236×10^5	9.236×10^5	3.029×10^{11}	2.863×10^{11}	1.024×10^{-1}	1.119×10^{-1}	1.109×10^{-7}	1.211×10^{-7}
Raffinate	6.557×10^4	6.556×10^4	3.280×10^{16}	2.256×10^{16}	5.739×10^3	3.717×10^3	8.754×10^{-2}	5.670×10^{-2}
Volatile FPs	1.049×10^4	1.048×10^4	4.149×10^{14}	3.004×10^{14}	4.567×10^1	3.306×10^1	4.353×10^{-3}	3.154×10^{-3}
Sum	9.997×10^5	9.997×10^5	3.322×10^{16}	2.286×10^{16}	5.785×10^3	3.750×10^3		
U%	92.39%	92.39%	0.00%	0.00%	0.00%	0.00%		
Raffinate%	6.56%	6.56%	98.75%	98.68%	99.21%	99.12%		
Volatile FPs%	1.05%	1.05%	1.25%	1.31%	0.79%	0.88%		

As can be seen from the results presented in Table 1, partitioning U from the remaining components of SNF using the UREX process would result in the removal of 92.39% of the initial heavy metal mass for final disposal. The U stream alone (assuming no additional mass from compounds of U) is off sufficiently low activity to be reclassified as ILW, while still containing 0.938% ^{235}U—representing a more favourable feed for re-enrichment than natural U, should this approach be desired, or an appropriate isotopic mixture for fissioning in efficient reactors such as the CANDU design. These values do not appreciably change whether the SNF is cooled for 5 or 10 years before reprocessing. A reduction in activity would arise from the removal of U decay products, but these would begin to grow into the material upon storage. Pu is counted with the raffinate feed here.

The raffinate outputs from UREX represent 6.56% of the total initial heavy metal mass for disposal and practically all of the activity and decay heat. Cooling SNF for 10 years instead of 5 before reprocessing would result in a marked (35.3%) reduction in overall decay heat and thus solvent degradation and other operational challenges. If we assume that the conversion of the elements present in the raffinate to oxides would grant a loading in glass of 20 wt%, and a final wasteform density of 3.33 g/cm^3, this means that per initial ton of heavy metal, 328 kg of vitrified HLW is produced, taking up a volume of 0.0984 m^3, and with a corresponding specific heat output of 17.5 W/kg if cooled for 5 years, or 11.3 W/kg if cooled for 10 years.

3.3. Scenario 3: The PUREX Process

The PUREX process (Figure 4) is the current gold standard in SNF reprocessing and has been used for over six decades due to its effectiveness at selectively separating U and Pu from the MAs and nearly all FPs. PUREX would normally produce separate U and Pu feeds alongside a raffinate containing the FPs and MAs, but for the purposes of this work, we will assume that the Pu is co-partitioned with at least some U in order to maintain proliferation resistance [17]. The raffinate output is, as above, vitrified and containerised for storage until deep geological disposal in a GDF can be undertaken, while the U and Pu would be converted to MOX for further energy generation. The respective masses, activities, and decay heats of these two streams from our simulated HBU PWR SNF are presented in Table 2. For comparison with prior works, please see the data published in the extensive report by Wigeland et al. [24], where this scenario corresponds to EG13 (limited recycle of U/Pu with new enriched-U fuel in thermal critical reactors) or EG21 (continuous recycle of U/Pu with new enriched-U fuel in thermal critical reactors) outlined therein.

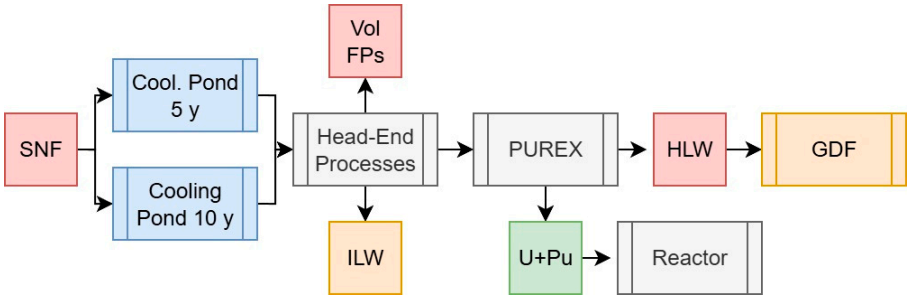

Figure 4. Simplified schematic summary of the PUREX process with SNF input and the primary outputs of these operations.

Table 2. Scenario 3 data, including feed masses, activities, decay heats, and specific decay heats. The values for the daughters of U are included with it.

	Masses (g/tiHM)		**Activity (Bq/tiHM)**		**Decay Heat (W/tiHM)**		**Specific DH (W/gHM)**	
Feed	5 y	10 y	5 y	10 y	5 y	10 y	5 y	10 y
U + Pu	9.364×10^5	9.361×10^5	6.392×10^{15}	5.086×10^{15}	3.253×10^2	3.107×10^2	3.47×10^{-4}	3.32×10^{-4}
Raffinate	5.280×10^4	5.313×10^4	2.641×10^{16}	1.747×10^{16}	5.414×10^3	3.407×10^3	1.03×10^{-1}	6.41×10^{-2}
Volatile FPs	1.049×10^4	1.048×10^4	4.149×10^{14}	3.004×10^{14}	4.567×10^1	3.306×10^1	4.35×10^{-3}	3.15×10^{-3}
Sum	9.997×10^5	9.997×10^5	3.322×10^{16}	2.286×10^{16}	5.785×10^3	3.750×10^3		
U%	93.67%	93.64%	19.24%	22.25%	5.62%	8.28%		
Raffinate%	5.28%	5.31%	79.51%	76.43%	93.59%	90.84%		
Volatile FPs%	1.05%	1.05%	1.25%	1.31%	0.79%	0.88%		

Reprocessing HBU PWR SNF using the PUREX process would remove at least 93.6% of the initial heavy metal mass for final disposal. In this context, we will not consider the U+Pu stream to be a waste, but rather a potential resource for the generation of further energy. If all of the U present is partitioned with Pu, the total concentration present would be equivalent to 1.38% if reprocessed after 5 years cooling, and 1.35% after 10 years, due to the decay of some 350 g of fissile ^{241}Pu. This presents a valid argument for the reprocessing of shorter-cooled (5 y) SNF for increased fuel cycle efficiency, given the higher fissile isotope content under these conditions and the general inefficiency of MA burning in thermal-spectrum reactors.

Given the relatively low Pu + ^{235}U content of the hypothetical fuel in this scenario, which could be effectively burned in a CANDU reactor or to lower burnups in a PWR, it would likely represent a more effective use of resources to partition a large proportion of the U from the U + Pu feed and instead form higher Pu content MOX (7–8% iHM) capable of reaching the same burnups as the initial UO_2 in Gen III(+) reactors [23]. The excess U partitioned off in this manner is at the same enrichment as described above and is suitable for re-enrichment for further power generation. It would be preferable to utilise any MOX produced as quickly as possible after reprocessing to mitigate the effects of ^{241}Am ingrowth into the fuel.

The presence of Pu in the U + Pu feed significantly increases both the activity and decay heat relative to the UREX U feed (Table 1), primarily due to the decay of ^{238}Pu, though, as this material is not intended for disposal, we do not need to pay too much consideration to these values. The specific decay heats relative to the HLW raffinate are approximately five orders of magnitude lower, primarily in the form of α-decay, though consideration would need to be paid to the significant neutron emission of ^{240}Pu and ^{242}Pu, the nuances of which are beyond the scope of this work.

The raffinate from PUREX represents 5.28% (5-year-cooled) or 6.31% (10-year-cooled) of the total initial heavy metal mass for disposal, alongside the majority (~77%) of the activity and 91–94% of the decay heat. As with UREX, cooling the SNF for 10 years instead of 5 before reprocessing results in a marked (37.1%) reduction in the decay heat of the HLW raffinate, and thus the potential radiolysis and other challenges induced during reprocessing. Assuming, as with above, a vitrified waste loading of 20 wt% and a final wasteform density of 3.33 g/cm^3, this means that per initial ton of heavy metal, 264 or 266 kg of waste would be produced after 5 and 10 years cooling, respectively, with a volume of 0.0795 m^3. These would have a specific heat output of 20.6 or 12.8 W/kg if cooled for 5 or 10 years before reprocessing, respectively.

3.4. Scenario 4: The PUREX Process with Minor Actinide Separations

The next evolution of SFR will likely build upon the PUREX process by the addition of MA separations, based upon the last several decades of research and industrial interest [17]. For the purposes of this scenario, we will assume a PUREX primary separation with a SANEX secondary separation removing the MAs (Np, Am, Cm, Bk, and Cf; Figure 5), though variations on this, such as the UK's conceptual Advanced PUREX process (which co-extracts Np with U and Pu for proliferation resistance) with an i-SANEX secondary separation (for Am and Cm), the European GANEX (U-only primary separation, transuranic secondary), or several of the more complex variations on the US UREX process, functionally achieve the same goal of segregating all of the actinides from the FPs. For comparison with prior works, please see the data published in the extensive report by Wigeland et al. [24], where this scenario corresponds to EG24 (continuous recycle of U/TRU with new natural-U fuel in fast critical reactors) outlined therein.

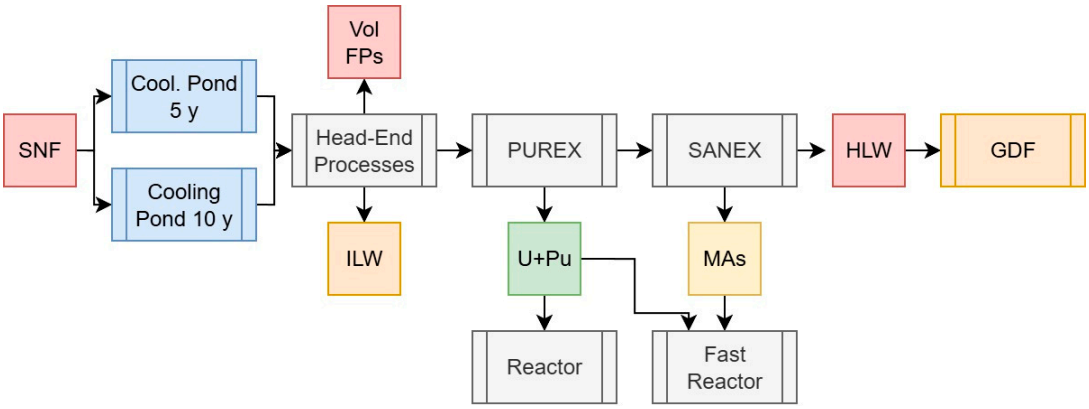

Figure 5. Simplified schematic summary of the PUREX + SANEX process with SNF input and the primary outputs of these operations.

We would assume for the purposes of this advanced fuel cycle implementation that any MAs are transmuted in a fast-spectrum reactor (e.g., sodium- or lead-cooled fast reactor), while the U/Pu MOX produced could be used to drive either thermal- or fast-spectrum reactors or as fast reactor driver fuel; Np can further be used as effective driver fuel in concert with Pu in fast reactors. The data are presented in Table 3. For the purposes of this scenario, we will assume that the REE feed produced by most MA separative flowsheets is routed back into the HLW raffinate.

Table 3. Scenario 4 data, including feed masses, activities, decay heats, and specific decay heats. The values for the daughters of U are included with it.

	Masses (g/tiHM)		Activity (Bq/tiHM)		Decay Heat (W/tiHM)		Specific DH (W/gHM)	
Feed	5 y	10 y	5 y	10 y	5 y	10 y	5 y	10 y
U + Pu	9.364×10^5	9.361×10^5	6.392×10^{15}	5.086×10^{15}	3.253×10^2	3.107×10^2	3.47×10^{-4}	3.32×10^{-4}
MAs	1.836×10^3	2.157×10^3	4.128×10^{14}	3.939×10^{14}	3.855×10^2	3.660×10^2	2.10×10^{-1}	1.70×10^{-1}
Raffinate	5.096×10^4	5.097×10^4	2.600×10^{16}	1.708×10^{16}	5.029×10^3	3.041×10^3	9.87×10^{-2}	5.97×10^{-2}
Volatile FPs	1.049×10^4	1.048×10^4	4.149×10^{14}	3.004×10^{14}	4.567×10^1	3.306×10^1	4.35×10^{-3}	3.15×10^{-3}
Sum	9.997×10^5	9.997×10^5	3.322×10^{16}	2.286×10^{16}	5.785×10^3	3.750×10^3		
U + Pu%	93.67%	93.64%	19.24%	22.25%	5.62%	8.28%		
MAs%	0.18%	0.22%	1.24%	1.72%	6.66%	9.76%		
Raffinate%	5.10%	5.10%	78.27%	74.71%	86.92%	81.07%		
Volatile FPs%	1.05%	1.05%	1.25%	1.31%	0.79%	0.88%		

The values for the U + Pu feed produced in this scenario are identical to those for the PUREX scenario outlined above and, as such, do not require any further discussion.

The additional MA feed generated increases in magnitude with increasing cooling times, primarily due to the decay of ^{241}Pu to ^{241}Am far outstripping the decay of any other isotopes (Cm primarily). This represents one of the primary drivers for reprocessing SNF at shorter cooling times, as the fissile content is higher, although, as discussed later, the impacts of ^{241}Pu decay on further energy production are limited. The MA feed represents 0.18 and 0.22% of the total heavy metal mass at 5 or 10 years cooling time, respectively, producing 19.25 or 22.25% of the activity, and 5.6 or 8.3% of the decay heat. If stored as dedicated MA oxides (MO_2, assuming an MW of 275), these materials would produce 0.19 or 0.15 W/g after 5 or 10 years' cooling, respectively, the reduction primarily arising from the decay of ^{244}Cm but offset partially by increased ^{241}Am concentrations. It is more likely, however, that these materials would be stored in a mixed oxide with U (typically 20% MAs), which would dilute the decay heat values by a factor of approximately five accordingly. Of necessary consideration, however, are the neutron emissions posed by Cm isotopes, which are significantly higher in magnitude than those of Pu and would perhaps necessitate only remote handling of Cm-containing fuel elements. This is, in part, the rationale in some nations for the development of Am-selective MA partitioning flowsheets for transmutation of only Am in fast-spectrum reactors or accelerator-driven systems [45].

The removal of the MAs from the HLW raffinate serves to reduce the mass for disposal (relative to UREX and PUREX) to 5.1% of the total heavy metal mass while decreasing both activity (75–78%) and decay heat (81–87%), depending upon cooling time. Reprocessing after 10 years instead of 5 years would result in a 39.5% reduction in HLW raffinate decay heat, an increase largely driven by the removal of the MAs. As with the other scenarios, if we assume a vitrified waste loading of 20 wt% and a final wasteform density of 3.33 g/cm^3, this means that per initial ton of heavy metal, there would be 254 kg of waste with a volume of 0.0762 m^3. These waste outputs would have a specific heat output of 19.74 or 11.94 W/kg after 5 or 10 years of cooling, respectively.

3.5. Scenario 5a: High-Heat Radionuclide Separations in PUREX with Minor Actinide Separations

The first of our novel scenarios is the addition of HHR separations to the PUREX+SANEX operations outlined above. Based upon our previous work [13–16], it is probable that these operations could be performed upstream of the primary and secondary separations via ion exchange processes, providing many benefits to operation and mitigations to operational challenges, as outlined in Figure 6. As the daughter products of ^{137}Cs and ^{90}Sr are key

contributors to the decay heat of the HHRs, these values are counted with their parents for the purposes of this scenario. The feed masses and decay heat data are presented in Table 4.

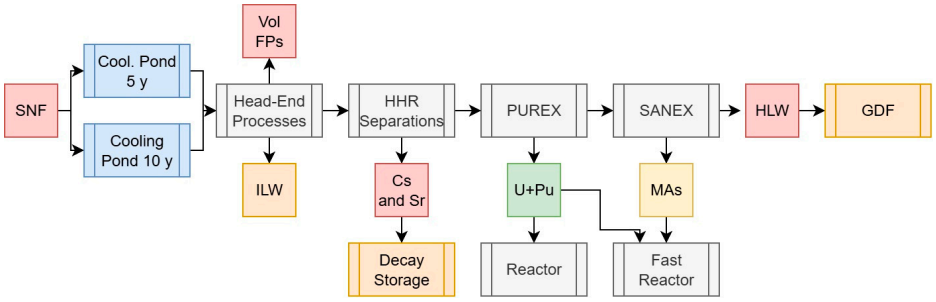

Figure 6. Simplified schematic summary of the PUREX + SANEX processes with SNF input and the primary outputs of these operations, combined with Cs+Sr HHR separations upstream of PUREX solvent extraction processes.

Table 4. Scenario 5a data, including feed masses, activities, decay heats, and specific decay heats. The values for the daughters of U are included with it.

	Masses (g/tiHM)		**Activity (Bq/tiHM)**		**Decay Heat (W/tiHM)**		**Specific DH (W/gHM)**	
Feed	5 y	10 y	5 y	10 y	5 y	10 y	5 y	10 y
Cs + Sr	6.157×10^{3}	5.806×10^{3}	2.017×10^{16}	1.612×10^{16}	3.961×10^{3}	2.930×10^{3}	6.43×10^{-1}	5.05×10^{-1}
U + Pu	9.364×10^{5}	9.361×10^{5}	6.392×10^{15}	5.086×10^{15}	3.253×10^{2}	3.107×10^{2}	3.47×10^{-4}	3.32×10^{-4}
MAs	1.836×10^{3}	2.157×10^{3}	4.128×10^{14}	3.939×10^{14}	3.855×10^{2}	3.660×10^{2}	2.10×10^{-1}	1.70×10^{-1}
Raffinate	4.480×10^{4}	4.517×10^{4}	5.834×10^{15}	9.566×10^{14}	1.068×10^{3}	1.106×10^{2}	2.38×10^{-2}	2.45×10^{-3}
Volatile FPs	1.049×10^{4}	1.048×10^{4}	4.149×10^{14}	3.004×10^{14}	4.567×10^{1}	3.306×10^{1}	4.35×10^{-3}	3.15×10^{-3}
Sum	9.997×10^{5}	9.997×10^{5}	3.322×10^{16}	2.286×10^{16}	5.785×10^{3}	3.750×10^{3}		
Cs + Sr%	0.62%	0.58%	60.70%	70.52%	68.46%	78.12%		
U + Pu%	93.67%	93.64%	19.24%	22.25%	5.62%	8.28%		
MAs%	0.18%	0.22%	1.24%	1.72%	6.66%	9.76%		
Raffinate%	4.48%	4.52%	17.56%	4.19%	18.46%	2.95%		
Volatile FPs%	1.05%	1.05%	1.25%	1.31%	0.79%	0.88%		

The values for the PUREX and MA feeds in this scenario will be identical to those presented above and, as such, warrant no further discussion. The separation of the HHRs Cs and Sr, however, significantly changes the considerations for raffinate handling in the back end of reprocessing operations.

After five years of cooling, the Cs and Sr collectively represent 0.62% of the initial heavy metal mass for disposal, whilst producing 61% of the activity and 68.5% of the decay heat. By 10 years, the mass contribution has fallen to 0.58%, whilst the activity and decay heat contributions have increased to 71% and 78.1% respectively.

As concentrating this amount of radioactivity to pure elements would represent significant operational and safety challenges if improperly engineered (see [46], we can at this stage conclude that any wasteform, or wasteforms accommodating Cs and/or Sr isolated from SNF, would have to be sufficiently "dilute": the specific decay heat of an elemental Cs-Sr wasteform would be 643 mW/g at 5 years cooling and 505 mW/g at 10 years, around that of pure elemental ^{238}Pu. At such "screaming" levels of activity, processes would require specific arrangements for active cooling and completely remote handling in heavily shielded hot cells. The details of these arrangements are beyond the scope of this work and have been discussed at length in our previous publications and presentations [13–16].

This approach would also present the opportunity to isolate a portion of the ^{137}Cs or ^{90}Sr and their daughters, both of which are useful isotopes in their own right [8]. Beyond this, recent research has the potential for H_2 production via water radiolysis, which could meet global demand at the time of writing from the radioactivity of present SNF stockpiles [10]. Removing >70% of the decay heat from dissolved SNF would reduce solvent radiolysis and its resulting challenges by a significant margin, as most of the β-γ emissions would have been eliminated from the process, thus having a benign effect on all downstream operations. The exact impacts of this are beyond the scope of this work but will be investigated in the future.

The HLW raffinate with Cs and Sr removed is a comparatively benign material, especially after being cooled for 10 years before reprocessing. This constitutes ~4.5% of the initial heavy metal mass for disposal, 17.5% or 5.2% of the activity after 5 or 10 years, and 18.4% or 3.0% of the total decay heat after the same lengths of cooling. At a vitrified waste loading of 20% and a final density of 3.33 g/cm^3, 225 kg of waste occupying 0.0675 m^3 would be produced for each tonne of initial heavy metal. This waste material would produce 4.76 W/kg after 5 years of cooling, falling to 0.49 W/kg after 10 years. This decline is a result of the majority of remaining emitters having shorter half-lives than ^{137}Cs and ^{90}Sr. While still appreciably heat-generating at 5 years, after 10 years of cooling, this raffinate could, with appropriate dilution, be cemented as ILW rather than vitrified (up to 6 wt% in cement with a density of 1.44 g/cm^3). Alternatively, the waste loading of vitrified forms could be increased, within the solubility limits of the glassy waste matrix, allowing for significant reductions in waste volumes and handling procedures in a departure from current NFC operations and traditions, while also potentially negating the need for deep geological disposal entirely if the Cs and Sr isotopes are utilised.

3.6. Scenario 5b: Platinum Group Metal Separations in PUREX with Minor Actinide Separations

The PGMs (Ru, Rh, Pd, and Ag) are likely the most valuable component of SNF after the actinides due to their high demand and natural scarcity. Unsurprisingly, their recovery has been proposed for several decades ([12], although these proposals have been tempered by the presence of several radioactive isotopes within each element. This means that PGMs recovered from SNF would either need to be cooled for several years (potentially decades, depending on activity limits (100 Bq/g), the values of which are likely too conservative [9], before use to allow these isotopes to decay or be used in remotely handled applications where the risk of radioactivity is minimal. Of the PGMs present, Pd is the most likely suitable for near-immediate use given the presence of one long-lived, low-energy isotope (^{107}Pd – $t_{0.5}$ = 6.5 My, Q_β = 34 keV). Fission platinum could be handled by industry in relative safety and used in applications such as H_2 storage or catalysis, aiding the Net Zero transition, or for the purification of H_2 produced from ^{137}Cs radiolysis of water.

As the chemistry of the PGMs is somewhat variable, dissolution in the head of SNF reprocessing is incomplete, and their partitioning throughout various current and proposed flowsheets can be chaotic, quantitative recovery would likely be challenging. It is likely best targeted by either post-PUREX or post-MA separations, where the bulk of the dissolved actinides have been removed and would thus not interfere with operations. In any case, a combination of methods is likely required, the nuances of which are beyond the scope of this work [22]. This addition to the previously explored flowsheet is presented in Figure 7, with the masses, activities, and decay heats for each feed in Table 5.

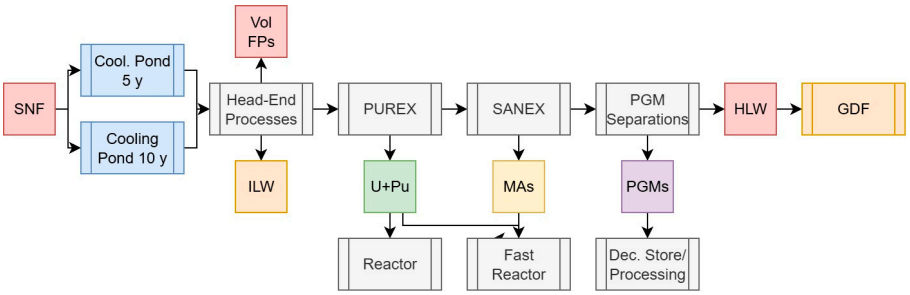

Figure 7. Simplified schematic summary of the PUREX + SANEX process with SNF input and the primary outputs of these operations, combined with back-end recovery of the PGMs from HLW raffinate. More complex approaches to PGM separations have been investigated elsewhere [22].

Table 5. Scenario 5b data, including feed masses, activities, decay heats, and specific decay heats. The values for the daughters of U are included with it.

	Masses (g/tiHM)		**Activity (Bq/tiHM)**		**Decay Heat (W/tiHM)**		**Specific DH (W/gHM)**	
Feed	5 y	10 y	5 y	10 y	5 y	10 y	5 y	10 y
U + Pu	9.364×10^5	9.361×10^5	6.392×10^{15}	5.086×10^{15}	3.253×10^2	3.107×10^2	3.47×10^{-4}	3.32×10^{-4}
MAs	1.836×10^3	2.157×10^3	4.128×10^{14}	3.939×10^{14}	3.855×10^2	3.660×10^2	2.10×10^{-1}	1.70×10^{-1}
PGMs	7.634×10^3	7.634×10^3	1.972×10^{15}	6.544×10^{13}	5.699×10^2	1.890×10^1	7.47×10^{-2}	2.48×10^{-3}
Raffinate	4.333×10^4	4.334×10^4	2.403×10^{16}	1.701×10^{16}	4.459×10^3	3.022×10^3	1.03×10^{-1}	6.97×10^{-2}
Volatile FPs	1.049×10^4	1.048×10^4	4.149×10^{14}	3.004×10^{14}	4.567×10^1	3.306×10^1	4.35×10^{-3}	3.15×10^{-3}
Sum	9.997×10^5	9.997×10^5	3.322×10^{16}	2.286×10^{16}	5.785×10^3	3.750×10^3		
U + Pu%	93.67%	93.64%	19.24%	22.25%	5.62%	8.28%		
MAs%	0.18%	0.22%	1.24%	1.72%	6.66%	9.76%		
PGMs%	0.76%	0.76%	5.94%	0.29%	9.85%	0.50%		
Raffinate%	4.33%	4.34%	72.33%	74.42%	77.07%	80.57%		
Volatile FPs%	1.05%	1.05%	1.25%	1.31%	0.79%	0.88%		

The U + Pu and MA feeds are the same as for Scenario 4 and do not warrant further discussion here. Quantitatively isolating the PGMs would result in 0.76% of the total initial heavy metal mass being partitioned away from the HLW raffinate, representing 5.9% of the activity at 5 years cooling and 0.3% at 10. This represents 9.85% and 0.5% of the decay heat at the same time intervals, with reductions primarily arising from the decay of ^{106}Ru ($t_{0.5}$ = 372 d). As the PGMs form stable, low-reactivity bulk metals, this represents the best means of storing these materials until either their radioactivity has decayed to acceptable levels or use is desired. If isolated in this form after 5 y cooling, the PGMs would produce 74.7 mW/g of decay heat or 2.48 after 10 y. This marked reduction in decay heat and activity represents a logical rationale for waiting to recover the PGMs from SNF, but if target isotopes (e.g., ^{106}Ru/^{106}Rh) are desired, shorter cooling would be necessary to secure appreciable concentrations of these, and they represent one of the few rationales for reprocessing shorter-cooled fuels.

The removal of the PGMs from the HLW raffinate reduces the mass for disposal, relative to PUREX, to 4.33% of the total initial heavy metal mass while decreasing both activity (72.3–74.4% of total) and decay heat (77.1–80.6% of total) marginally, depending on cooling time. Reprocessing after 10 years instead of 5 would reduce the decay heat of this HLW raffinate by 33.9%, a lower value than for the other scenarios due to the segregation of Ru, a major contributor to decay heat at 5 years of cooling. As with the other scenarios, if we assume a vitrified waste loading of 20 wt% and a final wasteform density of

3.33 g/cm^3, this means that per initial ton of heavy metal, there would be 217 kg of waste with a volume of 0.0651 m^3. These waste outputs would have a specific heat output of 20.6 or 13.94 W/kg after 5 or 10 years of cooling, respectively, primarily driven by the presence of Cs and Sr isotopes and waste volume reduction arising from PGM removal. This would also mitigate the challenges arising from the known incompatibility of the PGMs and their compounds in vitrified wasteforms and the challenges that occur during the formation of these materials [47].

3.7. Scenario 5c: Partitioning of Low-Activity Rare Earth Elements in PUREX with Minor Actinide Separations

The REEs (Y, and La to Lu) represent a large proportion of the FPs present in SNF, in addition to being, like the PGMs, naturally scarce and in high demand for a plethora of industrial and commercial applications [8,20,48]. As the majority of MA separation processes also separate chemically similar REEs, this provides a relatively easy route to the recovery of these elements, although the presence of a large number of radionuclides means that some uses would be limited to remote operations if these can be conducted safely with the levels of radiation present. Although several of the REEs have no radioactive isotopes, chemically separating the elements to a high enough decontamination factor would likely push the capabilities of current industrial chromatographic technologies used to achieve this for natural materials, where the REEs occur together and are separated based on ionic radius [49]. Figure 8 presents a simplified approach whereby the REEs would be separated with the MAs and then processed separately into inactive and low-activity elements (labelled LA REEs) and highly active ones (labelled HA REEs). The associated feed values are presented in Table 6. This would not be straightforward for the early lanthanides, as adjacent elements may not be consistent with the low or high activity nature, as outlined below. Instead of relying on chromatographic methods to separate Ce from the remaining lanthanides, this element can be recovered using solvent extraction via an adapted TBP-based process, as Ce^{IV} behaves much like Pu^{IV} in its extractability into the PUREX solvent system [50]. As the REEs are not volatile, it is likely not feasible to selectively separate any radioactive elements present based on volatility; decay storage represents the best manner of handling any potentially hazardous species present. This approach could, however, be used to recover useful REE isotopes such as ^{147}Pm. Solvent extraction using ligands such as DEHPA, TODGA, or similar could also be utilised [51–53].

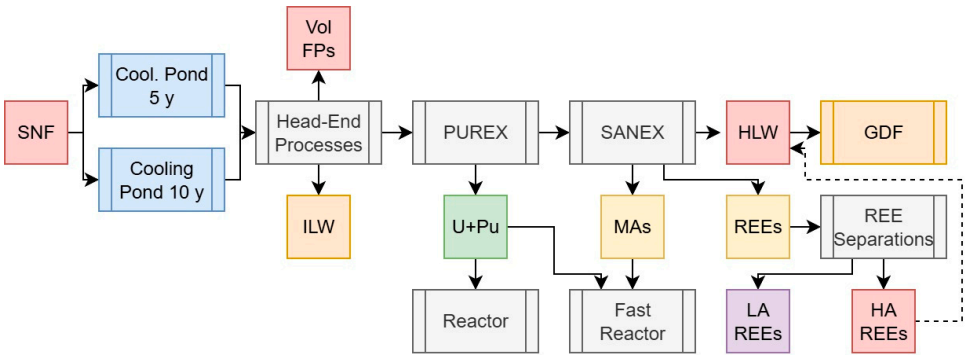

Figure 8. Simplified schematic summary of the PUREX + SANEX process with SNF input and the primary outputs of these operations with separations of the REEs into low- and high-active feeds for recovery and/or disposal respectively.

Table 6. Scenario 5c data, including feed masses, activities, decay heats, and specific decay heats. The values for the daughters of U are included with it.

	Masses (g/tiHM)		Activity (Bq/tiHM)		Decay Heat (W/tiHM)		Specific DH (W/gHM)	
Feed	5 y	10 y	5 y	10 y	5 y	10 y	5 y	10 y
U + Pu	9.364×10^5	9.361×10^5	6.392×10^{15}	5.086×10^{15}	3.253×10^5	3.107×10^2	3.47×10^{-4}	3.32×10^{-4}
MAs	1.836×10^3	2.157×10^3	4.128×10^{14}	3.939×10^{14}	3.855×10^2	3.660×10^2	2.10×10^{-1}	1.70×10^{-1}
REEs (LA)	1.251×10^4	1.250×10^4	1.666×10^{10}	3.715×10^8	1.269×10^{-3}	1.547×10^{-5}	1.01×10^{-7}	1.24×10^{-9}
REEs (HA)	5.041×10^3	5.059×10^3	3.731×10^{15}	8.519×10^{14}	4.824×10^2	8.717×10^1	9.57×10^{-2}	1.72×10^{-2}
Raffinate	3.341×10^4	3.342×10^4	2.227×10^{16}	1.622×10^{16}	4.546×10^3	2.953×10^3	1.36×10^{-1}	8.84×10^{-2}
Volatile FPs	1.049×10^4	1.048×10^4	4.149×10^{14}	3.004×10^{14}	4.567×10^1	3.306×10^1	4.35×10^{-3}	3.15×10^{-3}
HA REEs + Raff	3.845×10^4	3.848×10^4	2.600×10^{16}	1.708×10^{16}	5.029×10^3	3.041×10^3	1.31×10^{-1}	7.90×10^{-2}
Sum	9.997×10^5	9.997×10^5	3.322×10^{16}	2.286×10^{16}	5.785×10^3	3.750×10^3		
U + Pu%	93.67%	93.64%	19.24%	22.25%	5.62%	8.28%		
MAs%	0.18%	0.22%	1.24%	1.72%	6.66%	9.76%		
REEs (LA)%	1.25%	1.25%	0.00%	0.00%	0.00%	0.00%		
REEs (MA)%	0.50%	0.51%	11.23%	3.73%	8.34%	2.32%		
Raffinate%	3.34%	3.34%	67.04%	70.98%	78.59%	78.75%		
Volatile FPs%	1.05%	1.05%	1.25%	1.31%	0.79%	0.88%		

For the purposes of this work, the LA and HA REEs are separated by their parent element, with any daughters counted amongst the parent isotopes (e.g., ^{144}Ce and ^{144}Pr). The LA REEs are as follows:

1. Yttrium, accounting for the bulk stable, naturally occurring ^{89}Y and shorter-lived ^{88}Y and ^{91}Y. ^{90}Y is discounted, as this is the short-lived daughter of ^{90}Sr and would decay to extinction after several weeks.
2. Lanthanum, accounting for the two naturally occurring isotopes ^{138}La and ^{139}La, the former of which is slightly radioactive but primordial.
3. Praseodymium, accounting for the stable, naturally occurring ^{141}Pr. The short-lived, high-energy daughters of ^{144}Ce are discounted from this feed.
4. Neodymium, accounting for the stable and/or primordial, long-lived radioactive (primordial) isotopes ^{142}Nd, ^{143}Nd, ^{144}Nd, ^{145}Nd, ^{146}Nd, ^{148}Nd, and ^{150}Nd.
5. Gadolinium, terbium, dysprosium, holmium, erbium, thulium, and ytterbium, representing the upper limit of fission yields decreasing across this series, all of which consist of mostly stable isotopes with very small fractions of radioactive species.

And the HA-REEs:

1. Cerium, primarily from the decay of ^{144}Ce and its short-lived daughter ^{144}Pr, whose values are counted with this feed but would have decayed completely after ~20 y following removal from a reactor.
2. Promethium, all of the isotopes of which are radioactive, with the longest half-life present in any significant quantity being ^{147}Pm ($t_{0.5}$ = 2.62 y).
3. Samarium, which contains large quantities of the medium-lived ($t_{0.5}$ = 90 y) isotope ^{151}Sm, though the decay energy of this species is sufficiently low (76.7 keV), and is used in remote applications (i.e., catalysis), may be feasible.
4. Europium, which contains quantities of the radioactive medium-lived isotopes ^{150}Eu, ^{154}Eu, and ^{155}Eu.

As with the other scenarios, the U + Pu and MA feeds remain constant and do not warrant any further comment here. The LA REEs represent 1.25% of the total initial heavy metal mass, while the HA ones cover 0.50%.

Separating the REEs into LA and HA elements for use and disposal, respectively (notwithstanding the potential recovery of useful isotopes), poses several factors that must be considered. The HA REE feed would likely be best partitioned back into the HLW raffinate for vitrification and disposal, given the presence of several medium- and long-lived isotopes, meaning that any wasteform containing these elements alone would still be appreciably heat generating and thus not suitable for a cementitious wasteform. Most of the LA REEs could be released after several years of storage, if not immediately, depending upon the level of purity obtained during the operational separation(s).

Removing the LA REEs from the HLW raffinate stream reduces the mass for disposal relative to PUREX to 3.84% of the total initial heavy metal mass while having a negligible effect on both the percentage of activity and decay heat. Reprocessing after 10 years instead of 5 would reduce the HLW raffinate decay heat by 39%. If, as with the other scenarios, we assume a vitrified waste loading of 20 wt% and a wasteform density of 3.33 g/cm^3, per initial ton of heavy metal, 193 kg of waste with a volume of 0.0579 m^3 would be generated. These wastes would generate a specific heat output of 26.2 or 15.8 W/kg after 5 or 10 years of cooling, respectively, driven primarily by Cs and Sr isotopes and the significant volume reduction afforded by removal of the LA REEs.

3.8. Comparison of Waste Outputs from Different Spent Fuel Reprocessing Strategies

Table 7 and Figure 9 present a summary of the primary waste outputs from the different scenarios explored in this work with comparisons, where possible, to previous studies [24].

Table 7. Summary of HLW raffinate vitrified wastes per ton of initial heavy metal. The SNF+HLW masses associated with the various scenarios from Ref. [24] [a] are included for comparison. The normalised values are presented as bracketed percentages adjacent to these.

Scenario	SNF+HLW Mass (t/GWe.y) [a]	Mass (kg/tiHM)	Volume (m^3/tiHM)	Dec. Heat (W/kg, 5 y)	Dec. Heat (W/kg, 10 y)
1 (Open Fuel Cycle)	21.92 (100%, EG01)	1446 (100%)	>1.21	6.61	2.59
2 (UREX)	-	328 (22.6%)	0.0984	17.5	11.3
3 (PUREX)	3.42 (15.6%, EG13) 1.46 (6.7%, EG21)	264–266 (18.3–18.5%)	0.0795	20.6	12.8
4 (PUREX + SANEX)	1.34 (6.1%, EG24)	254 (17.5%)	0.0762	19.7	11.9
5a (PUREX + SANEX + HHR)	-	225 (15.5%)	0.0675	4.76	0.49
5b (PUREX + SANEX + PGM)	-	217 (15.0%)	0.0651	20.6	13.9
5c (PUREX + SANEX + REE)	-	193 (13.2%)	0.0579	26.2	15.8

The values generated by this work pose an interesting series of conclusions with respect to waste volumes. The open fuel cycle (Scenario 1) is highly unfavourable from a sustainability viewpoint, uses a high GDF volume in the worst case, and disposes of the largest mass, including a large amount of critical materials necessary to retain the SNF bundles indefinitely.

We do not observe the same variation in mass presented by Wigeland et al., as the calculation methodologies are different: their values account for overall fuel cycle outputs per unit energy [24], whereas here we utilise only the reprocessing HLW outputs, but nonetheless, the data demonstrate that closing the fuel cycle is far preferable from a disposal mass and volume perspective. As FP partitioning is not analysed in the prior work, we can draw no further comparisons to the data presented here.

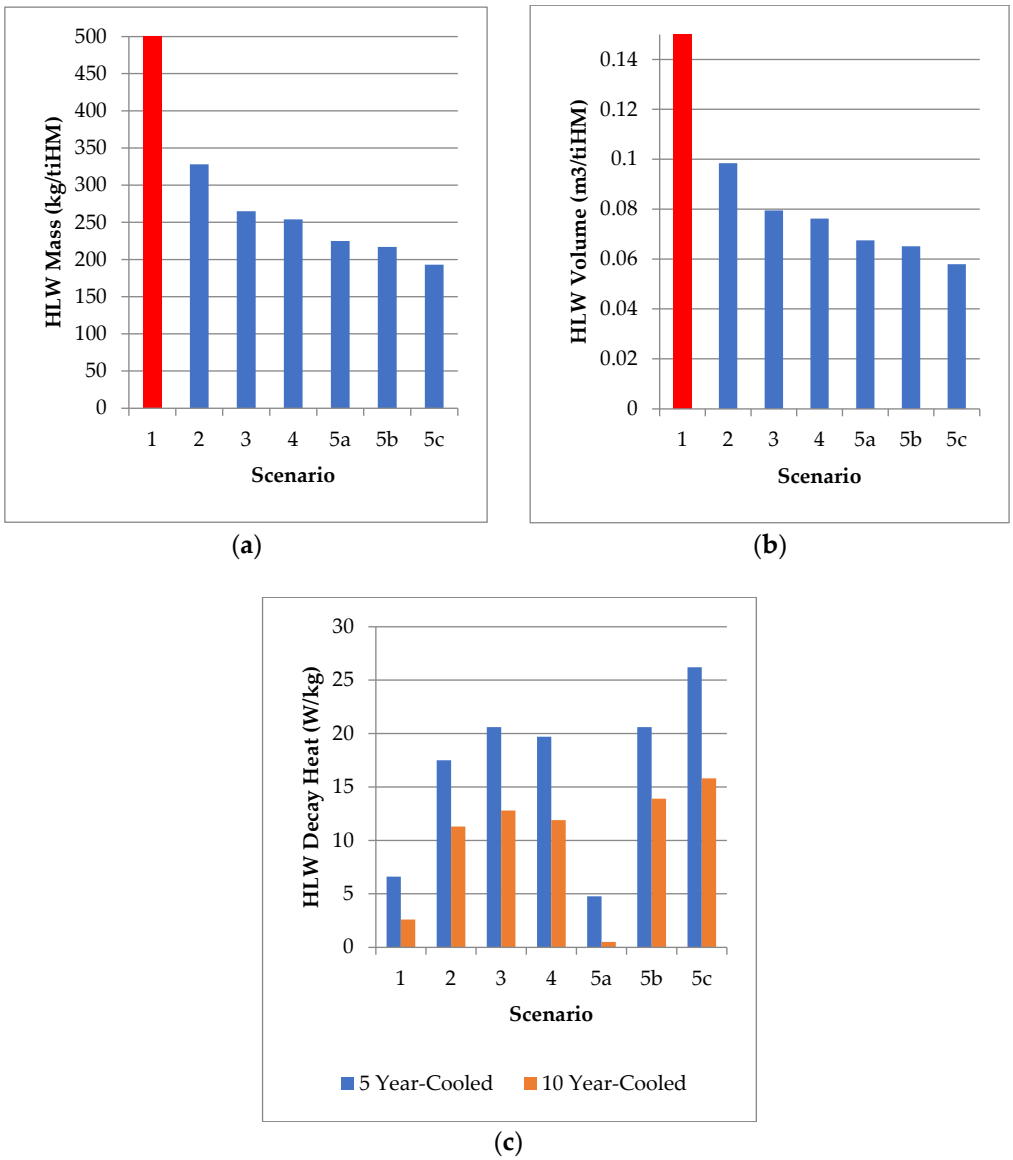

Figure 9. Graphical summary of HLW masses (**a**), volumes (**b**), and decay heats after 5 and 10 years of post-reactor cooling (**c**) from the SFR scenarios explored in this work. The Scenario 1 values are highlighted in different colours to represent the uncertainty around volume, mass, and decay heats. The values for mass and volume are greater than the scales presented by a significant margin, while the decay heats represent an upper bound depending upon the casks used for disposal.

Any of the other scenarios reduce the waste volumes for disposal by at least a factor of 12 (UREX, Scenario 2) and up to a factor of more than 20 (Scenario 5c). The proposed HHR separations (Scenario 4) have the potential, if implemented correctly, to otherwise eliminate the necessity for an HLW stream from SFR with sufficient cooling time, perhaps allowing for all remaining outputs to be reclassified as ILW with sufficient cooling time (at least 10 years post-reactor), though the exact specifications and storage media for a dedicated HHR repository or above-ground storage [11], decay storage facility, or usage for generating hydrogen from water by radiolysis [10] requires significant further research. Given the range of HLW glasses for long-term storage of vitrified wastes that have been explored, a combination of denser materials and higher loadings, where safe to do so, would reduce the waste volumes for disposal to a small fraction of that otherwise necessary.

The recovery of low-activity, high-value materials from SNF would further reduce waste volumes for disposal; for example, the combination of Scenarios 5a, 5b, and 5c, if all

co-implemented, would drop the raffinate volumes and radioactivity levels to values more amenably conducive to ILW processing, though this represents an idealised scenario where all possible resources are targeted and may not be economically feasible.

Our preliminary data simulating the re-use of the actinides recovered from the model fuel system used in this work indicate that there is little benefit to reprocessing SNF at 5 years instead of 10 with respect to further energy that can be generated, though this will be explored in future publications. This would arise as a proportion of fissile ^{241}Pu decays to ^{241}Am. The only other rationale for reprocessing fuels under 10 years is to recover shorter-lived isotopes with half-lives of a year or under (e.g., ^{106}Ru and ^{144}Ce) for use [8].

3.9. Direct and Indirect Value Recovery and Necessary Development

As previously stated, one of the primary detractors of nuclear reprocessing is the high costs. The potential for recovering valuable fission products as a means of offsetting this is not new but has only recently garnered any significant attention, considering the sustainability challenges surrounding the NFC. We can approximate the value recovery of high-value FP resources (i.e., PGMs and REEs) from SNF by multiplying their market prices with the masses present, assuming quantitative recovery and so forth, but discounting any considerations regarding processing, decay storage, and concerns surrounding the use of materials of radioactive origin that may impact on the perception of these materials. Obtaining relative values for the isotopes is a little more abstract and challenging, as this is derived from their use rather than the inherent value of the materials themselves. Nonetheless, we attempt to approximate this for Cs and Sr; the calculated value recovery from the PGMs and REEs is presented in Table 8, accounting for the likely final form and market values at the time of writing. Please note that these values are approximations, and a full socio-economic and environmental assessment of FP resource recovery and implementation is planned for future works, which are beyond the scope of the data presented here; these would constitute a sizable assessment of material reserves, demands, production capacities, industries, and the feasibility of separation from SNF during recycle operations. Please see the previous assessment of the French fuel cycle undertaken by Bourg and Poinssot as the most recent example [20] published to our knowledge, with cursory values of the platinoids in a Russian context reviewed by Pokhitonov [54]. Further recent overviews and more specific analyses of the candidate resources and categories thereof for recovery from SNF during recycle have been published [55]. Yet more pieces primarily discuss non-nuclear sources but suggest recovery from SNF should natural supplies dwindle [56].

The values presented in Table 8 give a total recoverable elemental value from Scenarios 5b and 5c, assuming co-implementation of 287 270 USD/tHM, not accounting for isotope values, the necessity for decay storage, processing, etc. For a 1000 tSNF/y reprocessing facility of similar scale to the UK's THORP plant, La Hague UP2 and UP3 in France, or Rokkasho in Japan, this would give a recoverable value of almost 300 M USD/y, providing a considerable offset to the operating costs of such a facility, assuming the costs of recovery, processing, and storage of such materials did not significantly otherwise impact operational costs. This does not include indirect costs saved by not having to dispose of these materials with HLW, as usually occurs. For the PGMs, the value is inherent and much greater than these indirect cost savings would be, but the inverse is true for the REEs—their volatile prices (lower at the time of writing than our previous work [22] mean that separation and recovery would mostly benefit downstream waste handling via volume reduction. The low concentrations of the heavier lanthanides mean that recovery of these, alongside silver, is likely not economically viable or worthwhile. In contrast, or rather in addition to the proposal of Vandenborre and co-workers [10], we would propose the utilisation of the

separated HRRs to generate hydrogen, as this would then free up actinides for further energy generation and likely decrease the size and cost and increase the efficiency of the radiolysis process. These will be thoroughly investigated in future works. The radiolytic production of hydrogen from water was also reviewed extensively by Leotlela [57], Ali and co-workers [58], and Agyekum and co-workers [59], with prior proposals published by Yoshida and co-workers [60]. Of the various proposals, that of Vandenborre and coworkers seems to be the best-developed at the time of writing [10].

Table 8. Values from REEs and PGMs recovered after 10 y of post-reactor cooling. Dollar values are in compound values; other figures are in elements per ton of heavy metal. The recovered values are adjusted to account for this. Values were acquired from https://www.dailymetalprice.com/metalprices.php?c=ru&u=kg&d and https://www.metal.com/price/Rare%20Earth/Rare-Earth-Oxides, as of 5 May 2025. See [54] for recent historical data.

Element/Form	Value (USD/kg)	Element Mass (g/tHM)	Activity (Bq/tHM)	Recovered Value (USD/tHM)
Ru (Ru)	20,094	4050	3.25×10^{13}	81,381
Rh (Rh)	172,810	719	3.29×10^{13}	124,250
Pd (Pd)	29,868	2720	7.83×10^{9}	81,241
Ag (Ag)	1065	149	1.63×10^{10}	157
Y (Y_2O3)	6.19	816	6.36×10^{-3} [a]	4
La (La_2O_3)	0.55	2170	3.88×10^{1}	1
Pr (Pr_2O_3)	52.30	1970	0 [b]	~80
Nd (Nd_2O_3)	51.69	7280	9.95×10^{1}	~300
Gd (Gd_2O_3)	19.66	259	8.55×10^{7}	4
Heavier Ln (M_2O_3, Tb, Dy, Ho, Er, Tm, Yb)	Various	7	2.86×10^{8}	<1

[a] Excluding ^{90}Y, as daughter of ^{90}Sr. [b] Excluding ^{144}Pr, as daughter of ^{144}Ce.

The indirect value that could be afforded from Scenario 5a in recovering Cs and Sr from SNF and utilising these isotopes for hydrogen production and heat generation, respectively, is potentially much greater in scope, especially for the latter [10]. This concept is fledgling at the time of writing, and as such requires significant further study before indirect value recovery from the use of Cs and Sr can be solidly specified, although, as Vandenborre and co-workers suggested, the current world SNF stockpile (~390,000 tons) would generate ~42.9 Mt of H_2 annually through their proposed radiolysis process. At a base H_2 price of 2 USD/kg, this would equate to around 86 bn USD production value per year. We would propose utilising these materials on the same nuclear-licenced site as a reprocessing facility and then shipping the hydrogen to where needed or storing it for energy generation on site (via fuel cell or turbine combustion) to permit load following. If the HHRs are not utilised in this manner, surface or dedicated repository decay storage separate from the remaining ILW, as proposed by Forsberg, would likely represent the best means of disposition [11].

With respect to the technological maturity of the proposed FP recovery scenarios, REE recovery is the most mature, as most MA separations also co-extract the chemically similar rare earths; Baron rated the technology readiness level (TRL) of most such processes at between 4 and 6 [17], with the commercial large-scale chromatographic separation of the REEs being well-established but not widely tested in a nuclear context. The back-end (post-solvent extraction of U, PU, and the MAs/REEs) separation of Cs and Sr has been assessed variously at TRL 4-8, while we would rate our own developmental head-end Cs separation at TRL 3 [13–15], and the Sr separation under such conditions at TRL 1 (purely

conceptual and untested). The recovery of the PGMs under SNF reprocessing conditions has been heavily reviewed in recent years and is at a similarly low (TRL 1-3) state of development [8,22,61,62]). Thus, the REE recovery would be the easiest to implement in a next-generation SNF plant but would yield the lowest direct value return and likely modest indirect value returns, Cs and Sr separations and utilisation require a relatively large amount of development for very significant indirect value returns, and PGM recovery needs a similar level of development for a large direct value return. Further value could be extracted from the volatile FPs driven off during SNF dissolution in the reprocessing head end as He, Kr, and Xe [8].

3.10. Implications for Future Reactors and Fuel Types

While the focus of this work has been on a simulant Gen III(+) reactor fuel, representing the most common kind of reactor under construction at the time of writing, and thus the most likely fuel system(s) that will be handled by any future SNF reprocessing facility, we will consider developing technologies and the implications of this in the context of this work.

At the time of writing, there are 52 operating Gen III(+) reactors with a similar number planned, under construction, or undergoing commissioning [63]. These reactors generate ~25 tSNF/y at typical loads, assuming an EPR-sized reactor, meaning 1300 tSNF generated annually for the current fleet, rising to double this figure within the next decade. The current stockpiles of HBU Gen III(+) fuel are thus likely in the region of 10–20,000 t, accounting for when the currently operating reactors of this generation began to come online.

The applicability of the proposed separations presented in this work will only increase as fuel burnups rise over time. These SNF systems will have higher concentrations of both valuable FPs and actinides for further energy generation, facilitating a fully closed NFC with Pu multi-recycle [25,26]. By recovering these, the costs of reprocessing could be offset directly and indirectly more so than with present (i.e., Gen II) and legacy SNF and available fissile inventory without further environmental impacts from mining of U. These, of course, would apply to long-cooled legacy fuel systems as well, which could possibly be run through a SNF reprocessing facility at higher throughput to better clear the large backlog of stored materials.

Novel fuel systems such as HALEU (high-assay low-enriched uranium, i.e., enriched between 5–20% ^{235}U) oxides and ATFs (advanced technology/accident tolerant fuels with advanced ceramics (e.g., UC, UN, U_3Si_2) and claddings (e.g., SiC, FeCrAl)) must be considered as well when proposing new separative technologies. Any future SNF reprocessing should be designed with a degree of "future proofing" to accommodate the higher fissile content of HALEU/high-MOX fuels, which would be more radioactive and thus either require longer post-reactor cooling before recycling or decay heat management, such as head-end HHR separations. Beyond this, the development of Gen IV reactors burning similar fuels (excluding TRISO) would also benefit from some of the additional processes proposed here. Further investigation of these newer fuels is, however, beyond the scope of this publication but will be studied in future works. Some data to support these studies are available [29].

4. Conclusions

The results presented in this work pose several interesting conclusions that warrant significant further consideration. While it has long been known that SFR reduces HLW volumes relative to SNF storage or direct disposal in the open fuel cycle, the potential for reclassification of primary HLW outputs to be reclassified down to ILW and cemented

instead of vitrified if the HHRs are removed poses a new paradigm for advanced NFCs that confirms our previously reported suspicions [13–15].

This could mean that the HLW portions of a GDF could be significantly diminished in size, if not eliminated entirely, saving a large capital investment otherwise needed for the fuel cycle. This is, of course, dependent on many other factors, such as the safe decay storage and/or utilisation of the Cs and Sr HHRs (e.g., for heat or H_2 generation [10], but has the potential, if correctly engineered and implemented, to revolutionise the NFC through generation of additional resources, passively, and cleanly. Co-implementing Scenarios 5a, 5b, and 5c would, of course, offer the greatest benefits in both radioactivity partitioning, waste volume reduction, and direct and indirect value recovery, but of these, the HHR separations presented in Scenario 5a are the most significant and impactful if these materials are appropriately utilised.

Treating SNF and all constituent parts as a resource, rather than waste, will allow us to greatly impact the economics, environmental impacts, and overall sustainability of the NFC for the long term, especially with current imperatives to decarbonise in the face of increased nuclear interest around the world [8], and the potential for fusion of Net Zero technologies [10].

Further investigations are required into a number of the questions highlighted in this work: how best to utilise the recovered actinides and in what reactor types; the extent to which partitioning and concentration of the HHRs could be best used for nuclear co-generation via H_2 production and/or heat recovery; and the extent to which combinations of resource recovery would further impact direct and indirect waste outputs from the NFC, amongst others. These will be investigated in future works, which will culminate in a thorough socio-economic and environmental life-cycle assessment of these concepts, including the effects on extended industries such as mining of precious materials (i.e., the PGMs and REEs). These future works will draw upon the extensive body of literature investigating fuel cycle options, including those cited here [24].

Supplementary Materials: The following supporting information can be downloaded at: https://www.mdpi.com/article/10.3390/jne6030029/s1, Source data Excel file.

Author Contributions: Conceptualization, H.E. and A.F.H.; methodology, A.F.H. and E.I.; software, A.F.H.; validation, A.F.H.; formal analysis, A.F.H.; investigation, A.F.H.; resources, A.F.H.; data curation, A.F.H.; writing—original draft preparation, A.F.H.; writing—review and editing, A.F.H., H.E. and E.I.; visualization, A.F.H.; supervision, A.F.H.; project administration, A.F.H. All authors have read and agreed to the published version of the manuscript.

Funding: This research received no external funding.

Data Availability Statement: The original contributions presented in this study are included in the article/Supplementary Material. Further inquiries can be directed to the corresponding author.

Acknowledgments: We wish to thank L. Stamford (University of Manchester) for the valued discussions in the preparation of this article.

Conflicts of Interest: The authors declare no conflicts of interest.

Appendix A

Table A1. Actinide and daughter product isotopes.

Element	Isotope(s)
Pb	^{206}Pb, ^{207}Pb, ^{208}Pb, ^{209}Pb, ^{210}Pb, ^{212}Pb
Bi	^{209}Bi, ^{210m}Bi, ^{210}Bi, ^{211}Bi, ^{212}Bi, ^{213}Bi, ^{214}Bi
Po	^{210}Po, ^{211}Po, ^{212}Po, ^{214}Po, ^{215}Po, ^{216}Po, ^{218}Po
At	^{217}At
Rn	^{219}Rn, ^{220}Rn, ^{222}Rn
Fr	^{221}Fr, ^{223}Fr
Ra	^{223}Ra, ^{224}Ra, ^{225}Ra, ^{228}Ra
Ac	^{225}Ac, ^{227}Ac, ^{228}Ac
Th	^{227}Th, ^{228}Th, ^{229}Th, ^{230}Th, ^{231}Th, ^{232}Th, ^{234Th}
Pa	^{231}Pa, ^{233}Pa, ^{234m}Pa, ^{234}Pa
U	^{232}U, ^{233}U, ^{234}U, ^{235}U, ^{236}U, ^{237}U, ^{238}U
Np	^{236}Np, ^{237}Np, ^{238}Np, ^{239}Np, ^{240m}Np
Pu	^{236}Pu, ^{238}Pu, ^{239}Pu, ^{240}Pu, ^{241}Pu, ^{242}Pu, ^{243}Pu, ^{244}Pu
Am	^{241}Am, ^{242m}Am, ^{242}Am, ^{243}Am, ^{245}Am
Cm	^{242}Cm, ^{243}Cm, ^{244}Cm, ^{245}Cm, ^{246}Cm, ^{247}Cm, ^{248}Cm, ^{250}Cm
Bk	^{249}Bk, ^{250}Bk
Cf	^{249}Cf, ^{250}Cf, ^{251}Cf, ^{252}Cf, ^{254}Cf
Es	^{254}Es, ^{255}Es

Table A2. Fission product isotopes.

Element	Isotope(s)	Element	Isotope(s)
Zn	^{66}Zn, ^{67}Zn, ^{68}Zn, ^{70}Zn	Sb	^{121}Sb, ^{123}Sb, ^{124}Sb, ^{125}Sb, ^{126}Sb
Ga	^{69}Ga, ^{71}Ga	Te	^{124}Te, ^{125}Te, ^{126}Te, ^{127m}Te, ^{128}Te, ^{129m}Te, ^{130}Te
Ge	^{70}Ge, ^{72}Ge, ^{73}Ge, ^{74}Ge, ^{76}Ge	I	^{127}I, ^{129}I
As	^{75}As	Xe	^{128}Xe, ^{129}Xe, ^{130}Xe, ^{131}Xe, ^{132}Xe, ^{134}Xe, ^{136}Xe
Se	^{76}Se, ^{77}Se, ^{78}Se, ^{79}Se, ^{80}Se, ^{82}Se	Cs	^{133}Ce, ^{134}Ce, ^{135}Ce, ^{137}Ce
Br	^{79}Br, ^{81}Br	Ba	^{134}Ba, ^{135}Ba, ^{136}Ba, ^{137m}Ba, ^{138}Ba
Kr	^{81}Kr, ^{82}Kr, ^{83}Kr, ^{84}Kr, ^{85}Kr, ^{86}Kr	La	^{138}La, ^{139}La
Rb	^{85}Rb, ^{87}Rb	Ce	^{139}Ce, ^{140}Ce, ^{141}Ce, ^{142}Ce, ^{144}Ce
Sr	^{84}Sr, ^{86}Sr, ^{88}Sr, ^{89}Sr, ^{90}Sr	Pr	^{141}Pr, ^{144}Pr
Y	^{88}Y, ^{89}Y, ^{90}Y, ^{91}Y	Nd	^{142}Nd, ^{143}Nd, ^{144}Nd, ^{145}Nd, ^{146}Nd, ^{148}Nd, ^{150}Nd
Zr	^{90}Zr, ^{91}Zr, ^{92}Zr, ^{93}Zr, ^{94}Zr, ^{95}Zr, ^{96}Zr	Pm	^{146}Pm, ^{147}Pm, ^{148m}Pm, ^{148}Pm
Nb	^{92}Nb, ^{93m}Nb, ^{93}Nb, ^{94}Nb, ^{95m}Nb, ^{95}Nb	Sm	^{146}Sm, ^{147}Sm, ^{148}Sm, ^{149}Sm, ^{150}Sm, ^{151}Sm, ^{152}Sm, ^{154}Sm,
Mo	^{95}Mo, ^{96}Mo, ^{97}Mo, ^{98}Mo, ^{100}Mo	Eu	^{150}Eu, ^{151}Eu, ^{152}Eu, ^{153}Eu, ^{154}Eu, ^{155}Eu
Tc	^{98}Tc, ^{99}Tc	Gd	^{152}Gd, ^{153}Gd, ^{154}Gd, ^{155}Gd, ^{156}Gd, ^{157}Gd, ^{158}Gd, ^{160}Gd
Ru	^{99}Ru, ^{100}Ru, ^{101}Ru, ^{102}Ru, ^{103}Ru, ^{104}Ru, ^{106}Ru	Tb	^{159}Tb, ^{160}Tb
Rh	^{102}Rh, ^{103m}Rh, ^{103}Rh, ^{106}Rh	Dy	^{160}Dy, ^{161}Dy, ^{162}Dy, ^{163}Dy, ^{164}Dy
Pd	^{102}Pd, ^{104}Pd, ^{105}Pd, ^{106}Pd, ^{107}Pd, ^{108}Pd, ^{110}Pd	Ho	^{165}Ho, ^{166m}Ho
Ag	^{107}Ag, ^{109m}Ag, ^{109}Ag, ^{110m}Ag	Er	^{166}Er, ^{167}Er, ^{168}Er, ^{170}Er
Cd	^{110}Cd, ^{111}Cd, ^{112}Cd, ^{113m}Cd, ^{113}Cd, ^{114}Cd, ^{116}Cd	Tm	^{169}Tm, ^{170}Tm, ^{171}Tm
In	^{115}In, ^{115m}In, ^{115}In	Yb	^{168}Yb, ^{169}Yb, ^{170}Yb, ^{171}Yb, ^{172}Yb
Sn	^{116}Sn, ^{117}Sn, ^{118}Sn, ^{119}Sn, ^{120}Sn, ^{122}Sn, ^{124}Sn, ^{126}Sn		

References

1. World Nuclear Association. World Nuclear Association. Radioactive Waste Management. WNA. 2002. Available online: https://world-nuclear.org/information-library/nuclear-fuel-cycle/nuclear-waste/radioactive-waste-management (accessed on 24 March 2025).
2. Holdsworth, A.F.; Ireland, E. Navigating the Path of Least Resistance to Sustainable, Widespread Adoption of Nuclear Power. *Sustainability* **2024**, *16*, 2141. [CrossRef]
3. Boscarino, J.E. From Three Mile Island to Fukushima: The impact of analogy on attitudes toward nuclear power. *Policy Sci.* **2019**, *52*, 21–42. [CrossRef]
4. *IAEA-TECDOC-1587*; Spent Fuel Reprocessing Options. International Atomic Energy Agency: Vienna, Austria, 2008. Available online: https://www-pub.iaea.org/MTCD/Publications/PDF/TE_1587_web.pdf (accessed on 24 July 2025).
5. IAEA Nuclear Energy Series NW-T-1.14 (Rev 1). *Status and Trends in Spent Fuel and Radioactive Waste Management, Annex I–VII*; International Atomic Energy Agency: Vienna, Austria. 2022; Available online: https://www-pub.iaea.org/MTCD/Publications/PDF/PUB1963_web.pdf and https://www-pub.iaea.org/MTCD/Publications/PDF/SupplementaryMaterials/PUB1963-ANNEXES-I-VII.pdf (accessed on 24 July 2025).
6. South Copeland GDF Community Partnership. International Focus: Sweden. 2024. Available online: https://southcopeland.workinginpartnership.org.uk/international-focus-sweden/ (accessed on 24 March 2025).
7. Sun, X.Y.; Han, L.H.; Li, X.X.; Hu, B.L.; Luo, W.; Liu, L. Transmutation of MAs and LLFPs with a lead-cooled fast reactor. *Sci. Rep.* **2023**, *13*, 1693. [CrossRef]
8. Holdsworth, A.F.; Eccles, H.; Sharrad, C.A.; George, K. Spent Nuclear Fuel—Waste or Resource? The Potential of Strategic Materials Recovery during Recycle for Sustainability and Advanced Waste Management. *Waste* **2023**, *1*, 249–263. [CrossRef]
9. Allison, W. We Should Stop Running Away from Radiation. *Philos. Technol.* **2011**, *24*, 193–195. [CrossRef]
10. Vandenborre, J.; Guillonneau, S.; Blain, G.; Haddad, F.; Truche, L. From nuclear waste to hydrogen production: From past consequences to future prospect. *Int. J. Hydrogen Energy* **2024**, *64*, 65–68. [CrossRef]
11. Forsberg, C.W. Rethinking High-Level Waste Disposal: Separate Disposal of High-Heat Radionuclides (^{90}Sr and ^{137}Cs). *Nucl. Technol.* **2000**, *131*, 252–268. [CrossRef]
12. Rohrmann, C.A. *Values in Spent Fuel from Power Reactors*; Report No. BNWL-25; Pacific Battelle Northwest Labs: Richland, WA, USA, 1965.
13. Bond, G.; Eccles, H.; Kavi, P.C.; Holdsworth, A.F.; Rowbotham, D.; Mao, R. Removal of Cesium from Simulated Spent Fuel Dissolver Liquor. *J. Chromatogr. Sep. Tech.* **2019**, *10*, 417.
14. Holdsworth, A.F.; Eccles, H.; Rowbotham, D.; Bond, G.; Kavi, P.C.; Edge, R. The Effect of Gamma Irradiation on the Ion Exchange Properties of Caesium-Selective Ammonium Phosphomolybdate-Polyacrylonitrile (AMP-PAN) Composites under Spent Fuel Recycling Conditions. *Separations* **2019**, *6*, 23. [CrossRef]
15. Holdsworth, A.F.; Eccles, H.; Rowbotham, D.; Brookfield, A.; Collison, D.; Bond, G.; Kavi, P.C.; Edge, R. The Effect of Gamma Irradiation on the Physiochemical Properties of Caesium-Selective Ammonium Phosphomolybdate–Polyacrylonitrile (AMP–PAN) Composites. *Clean. Technol.* **2019**, *1*, 294–310. [CrossRef]
16. Holdsworth, A.F.; Eccles, H.; George, K.; Sharrad, C.A. Heterogeneous Separations of Highly Active Radionuclides for Advanced Decay Heat & Waste Management in Next-Generation Spent Fuel Recycling/Reprocessing. In Proceedings of the 4th Cloud Conference: Nuclear Waste Management and Disposal, Virtual, 9 July 2020.
17. Baron, P.; Cornet, S.M.; Collins, E.D.; DeAngelis, G.; Del Cul, G.; Fedorov, Y.; Glatz, J.P.; Ignatiev, V.; Inoue, T.; Khaperskaya, A.; et al. A review of separation processes proposed for advanced fuel cycles based on technology readiness level assessments. *Prog. Nucl. Energy* **2019**, *117*, 24. [CrossRef]
18. Poinssot, C.; Rostaing, C.; Greandjean, S.; Boullis, B. Recycling the Actinides, The Cornerstone of Any Sustainable Nuclear Fuel Cycles. *Procedia Chem.* **2012**, *7*, 349–357. [CrossRef]
19. Sauer, M.C., Jr.; Hart, E.J.; Flynn, K.F.; Gindler, J.E.A. *Measurement of the Hydrogen Yield in The Radiolysis of Water by Dissolved Fission Products*; Report ANL-76-46; Argonne National Laboratory: Argonne, IL, USA, 1976.
20. Bourg, S.; Poinssot, C. Could spent nuclear fuel be considered as a non-conventional mine of critical raw materials? *Progr. Nucl. Ener.* **2017**, *94*, 222–228. [CrossRef]
21. Holdsworth, A.F.; Eccles, H.; George, K.; Sharrad, C.A. Recovery of Strategic High-Value Fission Products from Spent Nuclear Fuel during Reprocessing. *EPJ Web Conf.* **2025**, *317*, 01004. [CrossRef]
22. Hodgson, B.J.; Turner, J.R.; Holdsworth, A.F. A Review of Opportunities and Methods for Recovery of Rhodium from Spent Nuclear Fuel during Reprocessing. *J. Nucl. Eng.* **2023**, *4*, 484–534. [CrossRef]
23. Ando, Y.; Takano, H. *Estimation of LWR Spent Fuel Composition*; Report: JAERI-Research-99-004; Japanese Atomic Energy Research Agency: Tokai, Japan, 1999.
24. Wigeland, R.; Taiwo, T.; Ludewig, H.; Todosow, M.; Halsey, W.; Gehin, J.; Jubin, R.; Juelt, J.; Stockinger, S.; Jenni, K.; et al. *Nuclear Fuel Cycle Evaluation and Screening—Final Report, FCRD-FCO-2014-000106 Report/INL/EXT-14-31465*; Idaho National

Lab: Idaho Falls, ID, USA, 2014. Available online: https://fuelcycleevaluation.inl.gov/SitePages/Home.aspx (accessed on 24 July 2025).
25. Taylor, R.; Bodel, W.; Stamford, L.; Butler, G. A Review of Environmental and Economic Implications of Closing the Nuclear Fuel Cycle—Part One: Wastes and Environmental Impacts. *Energies* **2022**, *15*, 1433. [CrossRef]
26. Taylor, R.; Bodel, W.; Butler, G.A. Review of Environmental and Economic Implications of Closing the Nuclear Fuel Cycle—Part Two: Economic Impacts. *Energies* **2022**, *15*, 2472. [CrossRef]
27. Taylor, R.; Bodel, W.; Banford, A.; Butler, G.; Livens, F. Sustainability of Nuclear Energy—A Critical Review from a UK Perspective. *Sustainability* **2024**, *16*, 10952. [CrossRef]
28. Holdsworth, A.F.; George, K.; Adams, S.J.; Sharrad, C.A. An accessible statistical regression approach for the estimation of spent nuclear fuel compositions and decay heats to support the development of nuclear fuel management strategies. *Prog. Nucl. Energy* **2021**, *141*, 103935. [CrossRef]
29. Carter, J.T.; Lulptak, A.J.; Gastelum, J.; Stockman, C.; Miller, A.; Bickford, R.; Goff, J.; Hohorst, J.; Smith, M. *Fuel Cycle Potential Waste Inventory for Disposition*; Report: FCR&D-USED-2010-000031 Rev 5; Savannah River National Lab: Aiken, SC, USA, 2012.
30. Elter, Z.; Balkestahl, L.P.; Branger, E.; Grape, S. Pressurized water reactor spent nuclear fuel data library produced with the Serpent2 code. *Data Brief* **2020**, *33*, 106429. [CrossRef]
31. IAEA. Live Chart of Nuclides. 2025. Available online: https://www-nds.iaea.org/relnsd/vcharthtml/VChartHTML.html (accessed on 25 March 2025).
32. NRC. Data Tables. 2025. Available online: https://www.nrc.gov/reading-rm/doc-collections/cfr/part071/part071-appa.html#71appa_table1a (accessed on 25 March 2025).
33. WISE Nuclear Data Viewer. 2024. Available online: https://www.wise-uranium.org/nucv.html?Pa-234m (accessed on 25 March 2025).
34. Collins, E.D.; Del Cul, G.D.; Moyer, B.A. Advanced Reprocessing for Fission Product Separation and Extraction. In *Advanced Separation Techniques for Nuclear Fuel Reprocessing and Radioactive Waste Treatment*; Woodhead Publishing: Cambridge, UK, 2011; pp. 201–228.
35. Plumb, G.R. The management of gaseous wastes from reprocessing containing volatile fission products. *Prog. Nucl. Energy* **1984**, *13*, 63–74. [CrossRef]
36. Connelly, A.J.; Hand, R.J.; Bingham, P.A.; Hyatt, N.C. Mechanical properties of nuclear waste glasses. *J. Nucl. Mater.* **2011**, *408*, 188–193. [CrossRef]
37. Harrison, M.T. Vitrification of High Level Waste in the UK. *Proced. Chem.* **2014**, *7*, 10–15. [CrossRef]
38. Vienna, J.D. (Ed.) *Closed Fuel Cycle Waste Treatment Strategy, Fuel Cycle Research and Development*; Report: PNNL-2114; Pacific Northwest National Laboratory: Richland, WA, USA, 2015.
39. National Academies of Sciences, Engineering, and Medicine (NASEM). *Merits and Viability of Different Nuclear Fuel Cycles and Technology Options and the Waste Aspects of Advanced Nuclear Reactors*; The National Academies Press: Washington DC, USA, 2022. [CrossRef]
40. National Research Council (NRC). *Waste Forms Technology and Performance: Final Report*; The National Academies Press: Washington DC, USA, 2011. [CrossRef]
41. Vandegrift, G.F.; Regalbuto, M.C.; Aase, S.B.; Arafat, H.A.; Bakel, A.J.; Bowers, D.L.; Byrnes, J.P.; Clark, M.A.; Emery, J.W.; Falkenberg, J.R.; et al. Lab-scale demonstration of the UREX+ process. *Waste Manag.* **2004**, *4*, 1–22.
42. Acar, B.B.; Zabunoglu, H.O. Comparison of the once-through and closed nuclear fuel cycles with regard to waste disposal area required in a geological repository. *Annals Nucl. Ener.* **2013**, *60*, 172–180. [CrossRef]
43. Roddy, J.W.; Claiborne, H.C.; Ashline, R.C.; Johnson, P.J.; Rhyne, B.T. *Physical and Decay Characteristics of Commercial LWR Spent Fuel*; Report: ORNL/TM-9591/V1-R1; Oak Ridge National Laboratory: Oak Ridge, TN, USA, 1986; Available online: https://inis.iaea.org/records/g6231-89k58 (accessed on 24 July 2025).
44. Sky News: Inside the World's First Nuclear Waste Tomb in Finland. 2022. Available online: https://news.sky.com/story/inside-the-worlds-first-nuclear-waste-tomb-in-finland-12723295 (accessed on 26 March 2025).
45. Abderrahim, H.A.; Baeten, P.; Sneyers, A.; Schyns, M.; Schuurmans, P.; Kochetkov, A.; Van den Eynde, G.; Biarrotte, J.-L. Partitioning and transmutation contribution of MYRRHA to an EU strategy for HLW management and main achievements of MYRRHA related FP7 and H2020 projects: MYRTE, MARISA, MAXSIMA, SEARCH, MAX, FREYA, ARCAS. *EPJ Nucl. Sci. Technol.* **2020**, *6*, 33. [CrossRef]
46. Smith, D.R. Toy Engine, Radiation, Electricity: Shocking Facts from Early Days. OakRidger. 2013. Available online: https://eu.oakridger.com/story/opinion/columns/2013/01/29/toy-engine-radiation-electricity-shocking/49131693007/ (accessed on 6 July 2025).
47. Laurin, C.; Régnier, E.; Gossé, S.; Laplace, A.; Agullo, J.; Mure, S.; Brackx, E.; Toplis, M.; Pinet, O. Redox behavior of ruthenium in nuclear glass melt: Ruthenium dioxide reduction reaction. *J. Nucl. Mater.* **2021**, *545*, 152650. [CrossRef]

48. Natrajan, L.S.; Langford Paden, M.H. F-block Elements Recovery. In *Element Recovery and Sustainability*; Hunt, A., Ed.; Royal Society of Chemistry: Cambridge, UK, 2013; pp. 140–184.
49. Bruzzoniti, M.C.; Mentasti, E.; Sarzanini, C.; Braglia, M.; Cocito, G.; Kraus, J. Determination of rare earth elements by ion chromatography. Separation procedure optimization. *Anal. Chim. Acta* **1996**, *322*, 49–54. [CrossRef]
50. Carrott, M.; Flint, L.; Gregson, C.; Griffiths, T.; Hodgson, Z.; Maher, C.; Mason, C.; McLachlan, F.; Orr, R.; Reilly, S.; et al. *Spent Fuel Reprocessing and Minor Actinide Partitioning Safety Related Research at the UK National Nuclear Laboratory (No. NEA-NSC-R--2015-2)*; Nuclear Energy Agency: Paris, France, 2015.
51. Nascimento, M.; Valverde, B.M.; Ferreira, F.A.; Gomes, R.D.C.; Soares, P.S.M. Separation of Rare Earths by Solvent Extraction Using DEHPA. *REM Rev. Esc. Minas* **2015**, *68*, 427–434. [CrossRef]
52. Husain, M.; Ansari, S.A.; Mohapatra, P.K.; Gupta, R.K.; Parmar, V.S.; Manchanda, V.K. Extraction chromatography of lanthanides using N, N, N′, N′-tetraoctyl diglycolamide (TODGA) as the stationary phase. *Desalination* **2008**, *229*, 294–301. [CrossRef]
53. Shimojo, K.; Kurahashi, K.; Naganawa, H. Extraction behavior of lanthanides using a diglycolamide derivative TODGA in ionic liquids. *Dalton Trans.* **2008**, *37*, 5083–5088. [CrossRef]
54. Pokhitonov, Y.A. Recovery of Platinoids from npp spent Nuclear Fuel and Outlook for Their Use. *Atom. Ener.* **2020**, *127*, 367–374. [CrossRef]
55. NEA. *Unlocking the Hidden Value of Nuclear Fuel: The Societal Benefits of Diverse Material Recycling*; OECD Publishing: Paris, France, 2025; Available online: https://www.oecd-nea.org/jcms/pl_99853/unlocking-the-hidden-value-of-nuclear-fuel-the-societal-benefits-of-diverse-material-recycling?details=true (accessed on 24 July 2025).
56. Weng, Z.; Jowitt, S.M.; Mudd, G.M.; Haque, N. A Detailed Assessment of Global Rare Earth Element Resources: Opportunities and Challenges. *Econom. Geol.* **2015**, *110*, 1925–1952. [CrossRef]
57. Leotlela, M.J. Radiolysis of water by α- and β-particles from spent nuclear fuel. *Rad. Phys. Chem.* **2024**, *216*, 111361. [CrossRef]
58. Ali, I.; Imanova, G.; Alharbi, O.M.L.; Hameed, A.M.; Siidiqui, M.N. Recent updates in direct radiation water-splitting methods of hydrogen production. *J. Umm Al-Qura Uni. Appl. Sci.* **2024**, *10*, 567–578. [CrossRef]
59. Agyekum, E.B.; Odoi-Yorke, F.; Abdullah, M.; Chowhury, P. Investigating the nexus between radiolysis using spent nuclear fuel and hydrogen production, with environmental safety considerations—A literature review. *Nucl. Eng. Des.* **2025**, *438*, 114048. [CrossRef]
60. Yoshida, T.; Tanabe, T.; Sugie, N.; Chen, A. Utilization of gamma-ray irradiation for hydrogen production from water. *J. Radioanal. Nucl. Chem.* **2007**, *272*, 471–476. [CrossRef]
61. Safiulina, A.M.; Borisova, N.E.; Karpyuk, E.A.; Ivanov, A.V.; Lopatin, D.A. Extraction of Palladium from Spent Nuclear Fuel Reprocessing Solutions. *Metals* **2024**, *14*, 133. [CrossRef]
62. Swain, P.; Mallika, C.; Srinivasan, R.; Prakash, B.; Ravikumar, K.; Ganesan, V.; Selvaraj, K.; Venkatesan, S. Separation and recovery of ruthenium: A review. *J. Radioanal. Nucl. Chem.* **2013**, *298*, 781–796. [CrossRef]
63. International Atomic Energy Agency (IAEA) PRIS (Power Reactor Information System). 2025. Available online: https://pris.iaea.org/pris/worldstatistics/underconstructionreactorsbycountry.aspx (accessed on 23 June 2025).